









## RESEARCH ARTICLE

# Fire transforms effects of terrestrial subsidies on aquatic ecosystem structure and function

Christopher B. Wall<sup>1</sup>  | Cody J. Spiegel<sup>1</sup>  | Evelyn M. Diaz<sup>1</sup> | Cindy H. Tran<sup>1</sup>  |  
 Alexia Fabiani<sup>1</sup> | Taryn Y. Broe<sup>1</sup>  | Elisabet Perez-Coronel<sup>1</sup>  | Sara L. Jackrel<sup>1</sup> |  
 Natalie Mladenov<sup>2</sup>  | Celia C. Symons<sup>3</sup>  | Jonathan B. Shurin<sup>1</sup> 

<sup>1</sup>Department of Ecology, Behavior and Evolution, Division of Biological Sciences, University of California, San Diego, California, USA

<sup>2</sup>Department of Civil Construction & Environmental Engineering, San Diego State University, San Diego, California, USA

<sup>3</sup>Department of Ecology, Behavior and Evolution, University of California, Irvine, California, USA

## Correspondence

Christopher B. Wall, Department of Ecology, Behavior and Evolution, Division of Biological Sciences, University of California, San Diego, CA, USA.  
 Email: [cwall@ucsd.edu](mailto:cwall@ucsd.edu)

## Funding information

National Science Foundation, Grant/Award Number: 2018058

## Abstract

Fire can lead to transitions between forest and grassland ecosystems and trigger positive feedbacks to climate warming by releasing CO<sub>2</sub> into the atmosphere. Climate change is projected to increase the prevalence and severity of wildfires. However, fire effects on the fate and impact of terrestrial organic matter (i.e., terrestrial subsidies) in aquatic ecosystems are unclear. Here, we performed a gradient design experiment in freshwater pond mesocosms adding 15 different amounts of burned or unburned plant detritus and tracking the chronology of detritus effects at 10, 31, 59, and 89 days. We show terrestrial subsidies had time- and mass-dependent, non-linear impacts on ecosystem function that influenced dissolved organic carbon (DOC), ecosystem metabolism (net primary production and respiration), greenhouse gas concentrations (carbon dioxide [CO<sub>2</sub>], methane [CH<sub>4</sub>]), and trophic transfer. These impacts were shifted by fire treatment. Burning increased the elemental concentration of detritus (increasing %N, %P, %K), with cascading effects on ecosystem function. Mesocosms receiving burned detritus had lower [DOC] and [CO<sub>2</sub>] and higher dissolved oxygen (DO) through Day 59. Fire magnified the effects of plant detritus on aquatic ecosystem metabolism by stimulating photosynthesis and respiration at intermediate detritus-loading through Day 89. The effect of loading on DO was similar for burned and unburned treatments (Day 10); however, burned-detritus in the highest loading treatments led to sustained hypoxia (through Day 31), and long-term destabilization of ecosystem metabolism through Day 89. In addition, fire affected trophic transfer by increasing autochthonous nitrogen source utilization and reducing the incorporation of <sup>15</sup>N-labeled detritus into plankton biomass, thereby reducing the flux of terrestrial subsidies to higher trophic levels. Our results indicate fire chemically transforms plant detritus and alters the role of aquatic ecosystems in processing and storing carbon. Wildfire may therefore induce shifts in ecosystem functions that cross the boundary between aquatic and terrestrial habitats.

This is an open access article under the terms of the [Creative Commons Attribution](https://creativecommons.org/licenses/by/4.0/) License, which permits use, distribution and reproduction in any medium, provided the original work is properly cited.

© 2023 The Authors. *Global Change Biology* published by John Wiley & Sons Ltd.

## KEYWORDS

dissolved organic carbon, plankton, productivity, pyrogenic, trophic transfer

## 1 | INTRODUCTION

Positive and negative feedbacks between ecosystems and the atmosphere represent significant sources of uncertainty when forecasting future climate scenarios. Melting sea ice and permafrost, and the expansion of wildfire and biotic disturbances (e.g., forest insect outbreaks, invasive species), may liberate more carbon to the atmosphere and reduce the capacity for terrestrial and aquatic ecosystems to serve as carbon sinks, unleashing vicious cycles of climate and ecosystem instability that accelerate further warming (Fei et al., 2019; Hicke et al., 2012; Natali et al., 2021; Zheng et al., 2021). Fires liberate terrestrial carbon and produce greenhouse gases (e.g., carbon dioxide [CO<sub>2</sub>], methane [CH<sub>4</sub>], nitrous oxide [N<sub>2</sub>O]) and aerosols that shape the radiative balance of the atmosphere (Bowman et al., 2009). Globally, CO<sub>2</sub> emissions from wildfires contribute 1.8 Gt of C year<sup>-1</sup> to the atmosphere (2000–2019) (Zheng et al., 2021), equivalent to 5% of net carbon emissions in 2021 (34.9 Gt CO<sub>2</sub>) (Liu, Deng, et al., 2022). As atmospheric pCO<sub>2</sub> continues to rise, climate models predict a combination of human behavior and land-use practices will act in positive feedback with rising global temperatures and anthropogenic climate change (Zheng et al., 2021) to increase the severity and frequency of wildfires (Jones et al., 2022; Liu et al., 2010; Pausas & Keeley, 2021).

Wildfires are important disturbances that structure biological communities and shape the ecological properties and biogeochemistry of terrestrial (McLauchlan et al., 2020) and inland aquatic ecosystems (Bixby et al., 2015) and the oceans (Tang et al., 2021). Wildfires generate recalcitrant pyrogenic materials (e.g., smoke, ash, woody debris) that destabilize soil structure and organic matter cycling and increase the flux of nutrients and organic materials into inland and coastal waters by erosion (Larsen et al., 2009; Lewis et al., 2019). The deposition of pyrogenic materials as detritus and aerosols can alter the biogeochemistry of waterways and fluvial networks (Ball et al., 2021) and contribute to marine phytoplankton blooms by increasing nutrient availability (Tang et al., 2021). The impact of fire disturbance on terrestrial systems depends on ecosystem type (i.e., wetland, grassland, riparian forest), fire severity and area burned, and it can show both acute and sustained effects on ecosystem function (McCullough et al., 2019; Paul et al., 2022; Santos et al., 2019). Fire mobilizes nutrients (nitrogen [N] and phosphorus [P]) and affects nutrient export and retention by producing partially combusted, recalcitrant pyrogenic materials (Bixby et al., 2015) that can have immediate and long term impacts on vegetation, soils, and watersheds (Dahm et al., 2015; Diemer et al., 2015; Rodríguez-Cardona et al., 2020). In burned stream areas (<1 year post-fire), wildfires increased dissolved organic carbon (DOC), dissolved organic nitrogen, fine-sediments, and particulate organic matter (POM) relative to unburned reference streams (Minshall

et al., 2001). Wildfire can also increase erosion and detritus deposition in waterways, altering microbial metabolism and biogeochemical cycling (Bladon et al., 2008; Santos et al., 2019), reducing water quality (i.e., elevated turbidity, DOC, aromaticity), and contributing to low-O<sub>2</sub> conditions with lethal consequences for aquatic organisms (Dahm et al., 2015; Ramberg et al., 2010). As such, fire represents a disturbance that precipitates rapid changes in ecosystem services and biodiversity both on land and in water with implications for global carbon cycling and biosphere feedbacks to climate change (McCullough et al., 2019; McLauchlan et al., 2020).

Wildfires alter the fate and impact of terrestrial organic matter in aquatic ecosystems. Terrestrial organic matter provides inorganic nutrients that support primary producers and organic substrates (i.e., dissolved organic matter [DOM]) for growth of heterotrophic microbes (Lennon, 2004), as well as humic organic compounds that absorb light and suppress photosynthesis (Solomon et al., 2015). For instance, burning can alter both the elemental stoichiometry and chemical composition of organic matter (plant litter and soils) (Butler et al., 2020; Pellegrini et al., 2021), impacting the lability and susceptibility of organic matter to microbial and photochemical transformation/degradation (Lennon & Pfaff, 2005; Obernosterer & Benner, 2004; Solomon et al., 2015). Fire effects on organic material propagate through forest food webs (Butler et al., 2021) and can also drive multi-year increases in nutrient and elemental concentrations in aquatic systems post-fire (Carignan et al., 2000). The chemical transformation of plant detritus by fire also influences the processing and decomposition of burned materials by heterotrophic microbes and macroinvertebrates (Rodríguez-Lozano et al., 2015), thereby altering the rate and efficiency of energy transfer through food webs. As a result, burned and unburned detritus may have distinct impacts on the metabolic balance and functioning of aquatic ecosystems that determine the fate of terrestrial organic matter and the biological properties of aquatic food webs.

Natural lentic systems (i.e., ponds and lakes) and artificial inland waters (i.e., reservoirs) account for 90% of the freshwater surface area globally, which, along with lotic systems (i.e., rivers and streams), represent significant sources of CO<sub>2</sub> and CH<sub>4</sub> to the atmosphere (Pilla et al., 2022). Subsidies—or the transfer of organisms, energy, or nutrients across ecosystem boundaries—are integral for aquatic and terrestrial systems (Lafage et al., 2019). The influx of subsidies from terrestrial plants (i.e., various forms of plant detritus and soils) into aquatic ecosystems can support ecosystem primary and secondary production (Cole et al., 2011), as well as support net heterotrophy and increase the emissions of greenhouse gases (Lennon, 2004). However, the combined recalcitrant and light attenuating properties of terrestrial-DOC can also reduce rates of nutrient turnover (Jones & Lennon, 2015) and the efficiency by which essential substances (i.e., carbon, nitrogen, fatty acids) are

transferred between phytoplankton and zooplankton (Karpowicz et al., 2021) and suppress biomass production (Karlsson et al., 2015), thereby affecting lake ecosystem function and nutrient cycling. Fluxes of allochthonous inputs after wildfires and floods may lead to enhanced browning, where silt and organic compounds further affect light attenuation, reduce chlorophyll (Whitney et al., 2015) and increase respiration, resulting in hypoxic or anoxic conditions (Dahm et al., 2015). These effects can further suppress microbial degradation and shift carbon cycling and turnover by increasing carbon storage in sediments (Isidorova et al., 2016). Lentic systems have longer residence times than lotic systems and may therefore be particularly vulnerable to fire disturbance relative to other waterways (McCullough et al., 2019). However, a comprehensive understanding of fire effects (and their chronology) on inland waters is lacking.

Here, we performed a gradient-design mesocosm (Cottingham et al., 2005) experiment to test the effects of terrestrial subsidies on experimental pond ecosystems and whether these effects were altered by burning. We ask how wildfire affects the fate and impact of terrestrial production in aquatic ecosystems and potential critical thresholds in the loading of plant material. Thirty 400L pond mesocosms received 15 different amounts of either burned or unburned plant detritus from two abundant California shrub and tree species (sage and willow) found in local nature reserves and nurseries. We measured ecosystem metabolism by the amplitude of daily cycles in dissolved oxygen (DO) concentrations, and concentrations of dissolved greenhouse gases ( $\text{CO}_2$ ,  $\text{CH}_4$ ) at the water surface. To assess the potential for fire to alter the assimilation and transfer of terrestrial material in aquatic food webs (Spencer et al., 2003), we isotopically labeled living sage plants with  $^{15}\text{N}$  prior to harvesting

and fire-treatment (burned or unburned) to measure plant-N incorporation into plankton biomass (i.e., % sage-derived  $^{15}\text{N}$ ), hereafter referred to as trophic transfer. We predicted detrital loading would have non-linear (hump-shaped) effects on ecosystem metabolism, stimulating production and respiration at low levels due to fertilization but suppressing them at higher levels where oxygen and light were depleted (Jones & Lennon, 2015). Because fire transforms the stoichiometry and organic chemistry of plant detritus (Butler et al., 2021), we predicted these non-linear functions to vary in magnitude and shape between the burned and unburned allochthonous sources, with fire reducing the trophic transfer of plant-N to zooplankton consumers.

## 2 | MATERIALS AND METHODS

### 2.1 | Experimental design

Thirty experimental mesocosms (400L) were used to test the influence of plant detritus loading and burning effects on aquatic ecosystems (Figure 1). Fifteen mesocosms received unique amounts of either burned or unburned plant detritus, with two control tanks receiving no plant material. We used a regression design to test for non-linear response surfaces in the dependent variables (Kreyling et al., 2018). In this design, fifteen mesocosms contained gradually increasing quantities of either burned or unburned plant material ranging from 0 to 400g of dried plant biomass, with stepwise increases in plant material ranging from 11% to 150% from one treatment level to the next. This design allowed us to test for non-linear

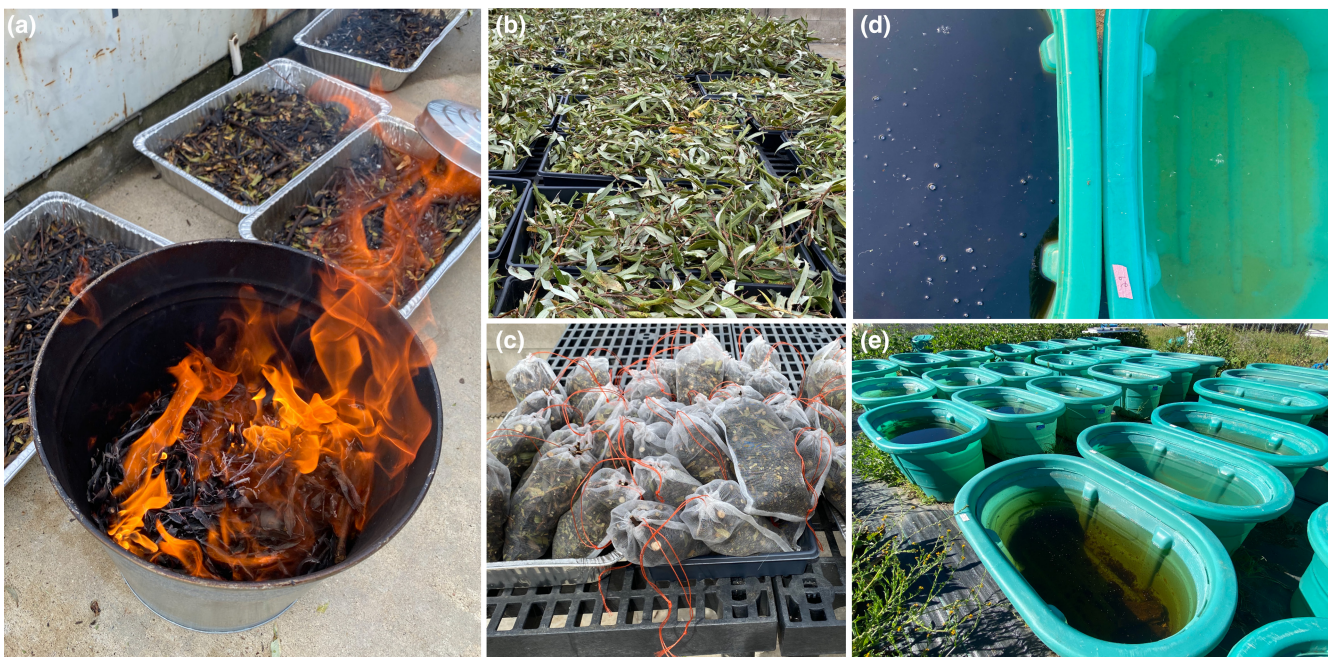


**FIGURE 1** Images showing (a) controlled burning of plant material, (b) dried-unburned plant material before and (c) after packed in mesh bags, (d) visual differences in water quality between tanks receiving high (left) and low (right) amounts of plant detritus, and (e) the experimental mesocosm array at the University of California San Diego Biology Field Station. (PC: CB Wall).

responses using a regression approach (Cottingham et al., 2005). The range in detrital loading was chosen based on preliminary tests on loading effects on water quality and to optimize the number or mesocosms within each treatment group. To account for water loss due to evaporation, water levels in the mesocosms were maintained by adding water from an adjacent 400L reservoir tank on a weekly basis. With the exception of mixing caused by periodic water additions, no attempts were made to stimulate flow, turnover, or to disturb detritus that settled at the bottom of tanks.

Each mesocosm was filled with municipal water (27 October 2021) and stocked with a concentrated mixture of live zooplankton (>63 $\mu$ m mesh) and residual phytoplankton collected from vertical tows at Lake Miramar, San Diego, CA (28 October, 5 November 2021). A sample of this concentrated >63 $\mu$ m zooplankton material was filtered onto a pre-combusted (2h, 550°C) 0.7 $\mu$ m GF/F filter and dried (60°C) for isotope analysis (detailed below). We used plant biomass from the shrub *Salvia leucophylla* (Greene) (hereafter, sage) and tree *Salix lasiolepis* (Benth.) (hereafter, willow) to generate the full target range of allochthonous loading. These species are native to Southern California and abundant in fire-prone scrub and woodland ecosystems in California and the Western United States. Twenty-three sage plants were purchased from a local nursery (9 June 2021) and grown in a 1:1 soil: vermiculite mixture in pots at the University of California San Diego Biology Field Station (La Jolla, CA).

On 24 June 2021 sage plants were watered with a single pulse (100mL) of 0.021 M  $^{15}\text{N}_4\text{Cl}$  in distilled water added to the base of the plants. Based on known and approximated molar nitrogen concentrations and  $^{15}\text{N}$ -enrichment in the  $\text{NH}_4\text{Cl}$  tracer and the soil mixture, we determined this pulse elevated soil  $^{15}\text{N}$  abundance to 6.4 atom %. Following the  $^{15}\text{N}$ -pulse, sage plants were grown for 60 days until harvest on 9 September 2021. Willow plant material was collected on 6 October 2021 from a stand of mature trees in the University of California Dawson Los Monos Reserve (Buena Vista, CA).

Sage and willow leaves and stems (<2cm diameter) were kept separate and air dried in a greenhouse for 24h, followed by an additional 24h in a drying oven (45°C). Once dried, plant biomass was cut into small pieces (<10cm) and divided into groups that either remained unburned or were exposed to fire. To simulate the non-uniform effects of wildfire on plant biomass, fire-treated plant material was exposed to varying degrees of burning at low and high burn severity, determined through visual assessment (Figure 1). Plant material (leaves and stems) was loaded into 75L aluminum containers and flamed with a handheld butane torch. To control the extent of burning, flames were extinguished with lids, with materials agitated and periodically turned over (Figure 1a). Both low and high severity burned plant materials were pooled according to plant species. In total, ~2kg of burned and unburned material was harvested for both sage and willow.

We analyzed plant isotopic ratios and elemental composition to evaluate the effects of fire on the starting plant materials added to mesocosms and the contribution of isotope tracer (i.e.,  $^{15}\text{N}$ ) to aquatic food webs. First, leaves (~5mg) from each species (sage

and willow) and treatments (burned and unburned) were separately ground and packed in tin capsules for C and N isotope analysis (see below). We then used leaves and woody stems of both burned and unburned sage and willow plant biomass to measure percent concentrations of nitrogen (N), sulfur (S), phosphorus (P), and potassium (K) and parts per million (ppm) concentrations of zinc (Zn) (A&L Western Laboratories, Modesto, CA).

Burned and unburned plant materials for each species were weighed and packed into leaf litter bags (25 $\times$ 15cm nylon bags of 250 $\mu$ m mesh size) to reduce buoyancy while also allowing for micro-invertebrate grazing and water flow through litter bags (Figure 1c). While this approach reduced any shadowing effects that mesocosms would have experienced from detritus at the water surface, litter packs were necessary to reduce unwanted dispersal of plant detritus among tanks. Each experimental mesocosm contained an equal mass of sage and willow for their respective fire-treatment (burned or unburned material), such that the lowest and highest plant biomass treatments (5 and 400g dry biomass added) received 2.5 or 200g of both willow and sage, respectively. On 5 November 2021, litter bags containing either burned or unburned plant detritus were placed into respective mesocosms; two tanks were left as controls where plankton were stocked but no plant materials were added.

## 2.2 | Sampling design and response metrics

Mesocosms were sampled five times during the experimental period: once at the start of the experiment before plant materials were added (Day 0; 3 November 2021), and four times after the addition of plants on 5 November 2021: Day 10 (15 November 2021), Day 31 (6 December 2021), Day 59 (3 January 2022), and Day 89 (2 February 2022).

Environmental parameters (temperature, DO, pH, conductivity) were measured throughout the study using a YSI Pro-Plus handheld multiparameter water sensor (YSI Inc., Yellow Spring, OH) calibrated against certified standards. During each discrete sampling period, measurements of DO concentration (% DO) were made three times over a 24h period (dawn-dusk-dawn) to calculate net primary productivity (NPP) and respiration (Resp) as the change in % DO from dawn to dusk (i.e., NPP) and dusk to dawn (i.e., Resp).

Isotope values were assessed in starting ground plant materials (dried leaves from burned and unburned sage and willow) and the concentrated >63 $\mu$ m plankton fraction from Lake Miramar ( $n=4-7$  for each). During the experiment, we measured isotope values in each mesocosm-tank at two time points (Days 10 and 31), assessing the seston (0.7–63 $\mu$ m)—consisting of particulate organic material (POM) and organisms (i.e., phytoplankton, rotifers)—and a zooplankton fraction (>63 $\mu$ m). Water samples were collected in each mesocosm with a 1-m integrated water sampler, filtered through a 63 $\mu$ m mesh separating the zooplankton and seston (hereafter, POM), and each fraction was filtered onto a pre-combusted (2h, 550°C) 0.7 $\mu$ m GF/F filter. Filters were wrapped in pre-combusted aluminum foil, frozen

(-20°C), and freeze-dried. Once dried, loaded biomass was scraped from the filter's surface (using 70%-ethanol cleaned razor blades) into a mortar and either cut with scissors or ground with a pestle before being packed into tin capsules for analysis. Approximately 10% of samples were run in duplicate, with duplicate samples differing by <3%. Measurement of nitrogen stable isotope values ( $\delta^{15}\text{N}$ ), carbon and nitrogen molar concentrations (C:N), and atom percent (atom-%  $^{15}\text{N}$ ) were made using an elemental analyzer-isotope ratio mass spectrometer (EA-IRMS) at the University of California Davis Stable Isotope Facility. Isotope values were compared using delta values ( $\delta$ ) using per mil (‰) notation relative to atmospheric  $\text{N}_2$  standards (air). Reproducibility of isotope abundance measurements was always within  $\pm 0.2\%$ .

Energy transfer from phytoplankton producers to zooplankton consumers can be measured by the flux of carbon (Karpowicz et al., 2021) or nitrogen (Barneche et al., 2021). We used plankton C:N molar concentrations at both sampling periods (Days 10 and 31) and across all mesocosms in both treatments to verify nitrogen assimilation was proportionate to carbon across times and treatments (i.e., no systematic change in C:N values) and within each plankton size fraction. We used a linear model to validate this assumption and found no effects of treatment ( $p = .915$ ) or sampling period (Days 10 and 31) ( $p = .783$ ) on plankton C:N, and POM/phytoplankton (<63  $\mu\text{m}$ ) C:N was higher than zooplankton (>63  $\mu\text{m}$ ), as has been shown previously ( $p < .001$ ) (Barneche et al., 2021) (Figure S1). Therefore, we used  $\delta^{15}\text{N}$  values of the two plankton size fractions as a measure of incorporation of  $^{15}\text{N}$ -labeled sage biomass into the aquatic food web.

Zooplankton feed on a variety of prey, including terrestrial material, however, the large overlap and small difference in isotope values between autochthonous and allochthonous sources complicate the estimation of allochthony from natural abundances (Cole et al., 2011). We therefore used  $\delta^{15}\text{N}$  values of  $^{15}\text{N}$ -labeled sage (nitrogen source 1 [ $\delta^{15}\text{N}$  of 296‰]) as one of two terrestrial sources (willow detritus was unlabeled,  $\delta^{15}\text{N}$  of 13‰), and the natural abundance  $\delta^{15}\text{N}$  values of the stock zooplankton mixture (nitrogen source 2 [ $\delta^{15}\text{N}$  of 11‰]) as a proxy for unlabeled autochthonous nutrients to determine the trophic transfer of nitrogen through aquatic food webs in a two-member mixing model (Post, 2002). The  $\delta^{15}\text{N}$  values of non-labeled willow ( $\delta^{15}\text{N}$  of 13‰) overlap with those of plankton at natural abundance collected from Lake Miramar ( $\delta^{15}\text{N}$  of 11‰) and POM measured in control mesocosms ( $\delta^{15}\text{N}$  of 7‰–15‰). Thus, mixing models represent the contribution of  $^{15}\text{N}$  entering plankton from sage alone and not from all terrestrial plant sources (including both sage and willow).  $^{15}\text{N}$ -labeled sage with  $\delta^{15}\text{N}$  values  $\sim 30\times$  higher than natural abundances of either plankton or unlabeled plant material allows us to clearly discriminate N that originated from sage and measure its uptake and incorporation by plankton as a function of supply and burning. To visualize  $^{15}\text{N}$ -sage incorporation into zooplankton biomass across the plant material gradient, we used the total plant-N added to tanks as a continuous predictor in a generalized additive model (see below), calculating N grams added by multiplying %N of materials (leaves and stems) analyzed at the start

of the experiment by the amount of plant biomass added to each mesocosm.

Water samples for DOC and total dissolved nitrogen (TDN) were collected at five timepoints using a 1-m integrated water sampler distributed across each tank; total dissolved phosphorus (TDP) was measured at one time point (Day 31). DOC and TDN water samples were filtered (pre-combusted 0.7  $\mu\text{m}$  GF/F filters), stored in pre-combusted borosilicate amber vials, and acidified (37% HCl) to a pH of 3. Mesocosm DOC and TDN were measured in the WIRLab at San Diego State University using a high temperature combustion method (Shimadzu TOC-L Total Organic Carbon and Total Nitrogen Analyzer) calibrated with potassium hydrogen phthalate standards (1–50 mg C/L, 1–10 mg N/L). Approximately 10% of samples were run in duplicate, with standard deviations of repeat-measurements falling within 10% of mean values. TDP was measured at the University of Hawai'i Hilo Analytical Laboratory on a Lachat QuikChem 8500 series 2 Flow-Injection Analyzer using USGS I-4650-03 for external digestion and US-EPA method 365.3 for phosphorus analysis (detection limit of 3.1  $\mu\text{g/L P}$ ).

## 2.3 | Greenhouse gas concentrations

Samples for  $\text{CO}_2$  and  $\text{CH}_4$  greenhouse gases were collected from each tank on Days 0, 10, 31 and 59 of the experiment using the headspace method (Perez-Coronel et al., 2021; Sobek et al., 2003). Background concentrations of  $\text{CO}_2$  and  $\text{CH}_4$  in ambient air were collected at each sampling day by collecting 12 mL of air in evacuated Exetainers (Labco Limited). In calculating Day 0 ambient air  $\text{CH}_4$  concentrations, background [ $\text{CH}_4$ ] in two ambient air sample blanks were contaminated (60% higher than the average background) and were discarded as outliers, being replaced with ambient  $\text{CH}_4$  concentrations at Day 10. Tank water temperatures were recorded and 25 mL of surface water (0.1 m depth) was collected in a sterile 60 mL syringe from each tank. An additional 25 mL of ambient air was collected into the same syringe. The syringe containing water and air was shaken for 2 min to reach equilibration and air was then injected into evacuated Exetainers for  $\text{CO}_2$  and  $\text{CH}_4$  quantification. Samples were stored upside down at room temperature and sent for analysis within 3 weeks to the University of California Davis Stable Isotope Facility.

Analysis of atmospheric  $\text{CO}_2$  was performed using a Thermo Scientific GasBench II coupled to a Thermo Finnigan Delta Plus XL isotope-ratio mass spectrometer. Analysis of atmospheric  $\text{CH}_4$  was performed on a Thermo Scientific GasBench II + PreCon trace gas concentration system coupled to a Thermo Scientific Delta V Plus isotope-ratio mass spectrometer. Molar concentrations of  $\text{CO}_2$  and  $\text{CH}_4$  in water were calculated based on headspace concentrations of  $\text{CO}_2$  (Weiss, 1974) and  $\text{CH}_4$  (Yamamoto et al., 1976) and gas solubilities using the appropriate temperature and atmospheric pressure corrected Henry's constant and accounting for the amount of  $\text{CO}_2$  or  $\text{CH}_4$  added by ambient air (Kokic et al., 2015). Unlike  $\text{CH}_4$ ,  $\text{CO}_2$  undergoes dynamic

chemical equilibrium with multiple carbonate species. In the absence of measurements of total alkalinity or dissolved inorganic carbon, quantification of CO<sub>2</sub> concentration using the headspace method can lead to poor resolution in undersaturated samples at low pCO<sub>2</sub> (Koschorreck et al., 2021). To account for carbonate equilibrium shifts, we use total alkalinity (mg CaCO<sub>3</sub>/L) estimates from source water in City of San Diego reservoirs with equilibrium and dissociation constants (Millero, 1979, 2010) to provide a more precise measure of CO<sub>2</sub> concentrations, following (Koschorreck et al., 2021). To express the percent saturation of molar concentrations CO<sub>2</sub> and CO<sub>4</sub> above concentrations of ambient air, we calculated the percent excess for each gas:  $\% \text{ excess} = \text{gas}_{\text{measured}} / \text{gas}_{\text{expected}} \times 100$ , where  $\text{gas}_{\text{measured}}$  is gas molar concentration in the headspace and  $\text{gas}_{\text{expected}}$  is gas concentration expected at atmospheric equilibrium. Percent excess values >100% indicate supersaturation and values <100% indicate undersaturation.

## 2.4 | Statistical analysis

A series of linear models and non-parametric tests were used to evaluate differences in δ<sup>15</sup>N values and C:N ratios across starting materials (willow, sage, plankton; leaves versus stems) and effects of burning treatments on starting plant materials. Using pooled values for burned and unburned leaves, Mann-Whitney *U*-tests evaluated differences in δ<sup>15</sup>N and C:N between the plant materials (<sup>15</sup>N-labeled sage versus non-labeled willow leaves) and non-labeled materials (willow versus the plankton stock). Burning effects on δ<sup>15</sup>N and C:N in sage leaves and willow leaves were evaluated in separate one-way linear models. A two-way linear model was used to test treatment (burned, unburned) and plant material type (leaves, stem) effects on sage and willow biomass (%N, %K, %P, %S, Zn ppm), with ANOVA tables generated using Type-III sum of squares in the *car* package (Fox & Weisberg, 2019).

The effects of treatment (burned and unburned) and plant detritus loading on the response variables were analyzed using generalized additive models (GAMs) in the *mgcv* package (Wood, 2011). Each time point was analyzed individually to account for the dynamic changes in response metrics over the course of the experiment since full models (i.e., the inclusion of all time points) introduced extreme concurvity. Within each time point, we applied GAMs in a model selection framework that compared three models: the 'simplest' model including only a single global smoother fit to all data; a model with a global smoother and a parametric 'Treatment' term, allowing different intercepts for burned and unburned treatments; and a model with a factor-smooth term which provided different smoothers for each treatment with a parametric term for treatment-specific intercepts. This approach allowed us to evaluate the relationship of response variables across the plant detritus gradient with the hypotheses that these relationships were non-linear and either offset according to treatments

and/or exhibited distinct treatment-specific structure (Pedersen et al., 2019).

Candidate models were compared using Akaike information criterion (AIC), and models with the lowest AIC value selected. GAMs were inspected for model concurvity using the 'concurvity' function in the package *gratia* (Simpson, 2022). Model fits were assessed using 'gam.check,' with ANOVA tables generated using 'anova.gam' in the *mgcv* package to provide Wald tests of significance for parametric and smooth terms. In all cases, differences between burned and unburned treatments were illustrated by plotting the "difference smooth" using 'plot\_difference' in *tidymv* (Coretta et al., 2022), which calculates the differences between smoothers of two conditions and determines regions of significance as areas where  $s(\text{treatment 1}) - s(\text{treatment 2})$  is greater than zero and does not include treatment-smooth confidence intervals. In model testing of <sup>15</sup>N-enrichment and the contribution of sage-<sup>15</sup>N to plankton, size fraction (i.e., <63 μm POM and >63 μm zooplankton) was also included as a parametric term for model selection. Plankton C:N were visualized using a GAM with size fraction as both a main effect and a factor-smooth term. All analyses were performed in R version 4.2.1 (R Core Team, 2022).

## 3 | RESULTS

### 3.1 | Elemental analyses

We observed differences in elemental concentrations in plant material among species, tissue types, and burning treatments, although the largest differences were between species and plant parts (Figure 2; Tables S1 and S2). Overall, burning reduced sage leaf %N by 8%, but increased stem %N (18%) and increased sage %K by 16%. Willow showed greater and more consistent shifts in elemental composition, with burning increasing %N, %P, and %K from 21%–43% and increasing %S and Zn ppm in leaves alone (18% and 148%, respectively) (Figure 2).

### 3.2 | Dissolved organic carbon

Prior to the addition of plant material DOC concentrations were low, averaging ~3 mg/L across all mesocosms. Following the addition of plant material, DOC increased to ~60 mg/L in the highest treatments (Figure 3). Detritus loading had significant non-linear effects on DOC concentrations throughout the experiment, and DOC concentrations showed distinct patterns among burned and unburned treatments. The relationship between detritus loading and DOC was strongest in the experiment when DOC concentration was highest (Days 10 and 31) but was reduced in subsequent samplings as DOC declined (Figure 3). The rise in DOC with detrital loading also differed among burned and unburned treatments at the first three time points (Days 10, 31, and 59) (Figure S2), as

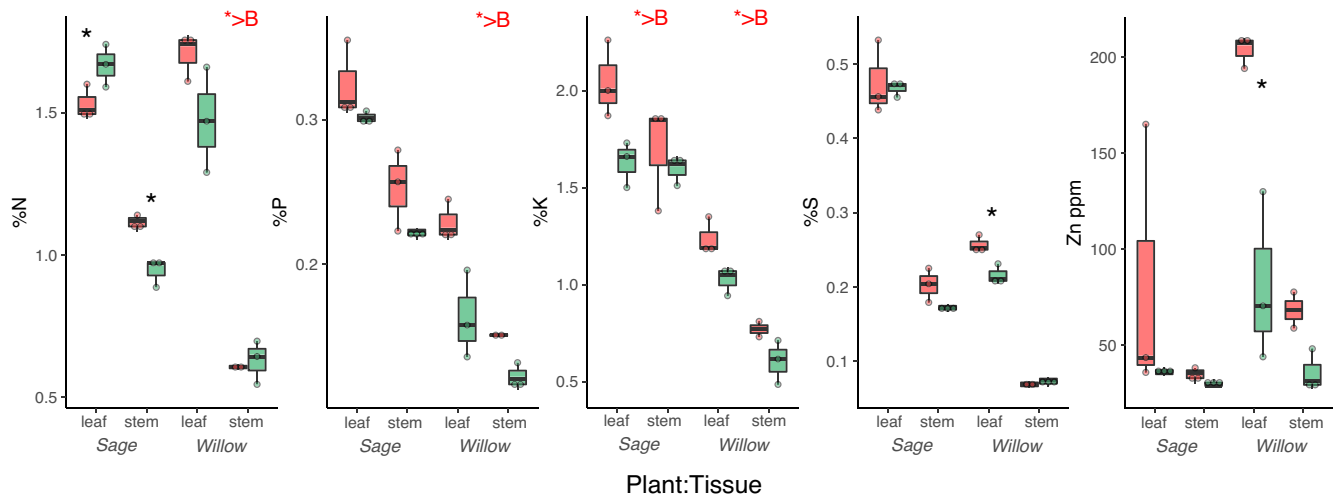


**FIGURE 2** Elemental analysis of burned (red, left) and unburned (green, right) plant material (leaf and stem) from sage and willow prior to being added to experimental treatments. Statistical models were run separately for sage and willow, with *black asterisks* indicating significant post-hoc comparisons ( $p < .05$ ) of burned effects within a plant:tissue type. Significant overall treatment effects (burned vs. unburned) for either sage or willow in the absence of interactions are shown with *red asterisks*, with symbols indicating higher values in burned treatments (>B). Box plots depict the median (bold center line), first and third quartiles (lower and upper bounds), whiskers (1.5 $\times$  the distance between first and third quartiles).

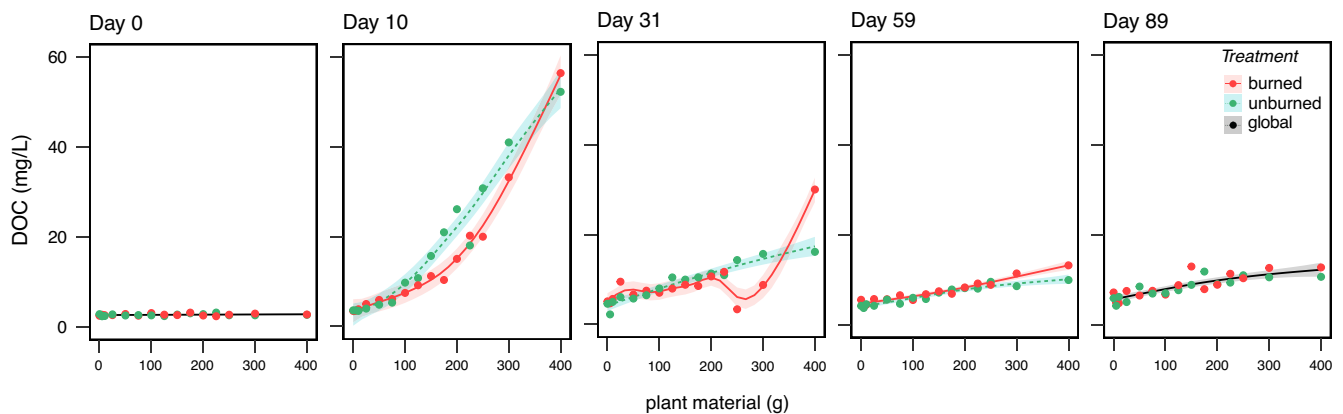


**FIGURE 3** Dissolved organic carbon (DOC) concentration in treatments receiving burned and unburned plant material at the beginning of the study (prior to adding materials [Day 0]) and across four experimental periods. Lines represent linear regression and generalized additive models with 95% confidence intervals. Black lines with gray confidence intervals indicate global smoothers across all data points; solid (burned) and dotted (unburned) colored lines indicate factor-smoothers that vary between treatments.

indicated by best-fit model AIC (Table S3) and differences between factor smoothers (Table S4). DOC was up to 42% lower in burned tanks receiving mid-range plant additions (~100–300g) at Day 10 and up to 76% lower at Day 31 (~200–300g). However, DOC at Day 31 spiked at the highest-loading tank (400g) being three-fold higher in the burned treatment relative to the unburned treatment. DOC remained elevated (30% greater) in burned tanks (~300–400g) through Day 59 (Figure 3; Figure S2). By the last sampling period (Day 89), DOC still showed a positive relationship with plant detritus loading, although this effect was small (total DOC range 4–12mg/L) and equivalent between burning treatments (Figure 3; Figure S2).

### 3.3 | Total dissolved nitrogen and phosphorus

The addition of plant material had significant non-linear effects on TDN that persisted through Day 89 (Figure S3). This shape of the non-linear relationship was similar between burned and unburned treatments at Day 10. Subsequently, burned and unburned treatments diverged and maintained statistical differences through Day 89. TDN tended to be lower in burned tanks at Day 31 ( $p = .053$ ) but was notably 56% higher on average for high-range (>200g) burned treatments at Day 59 and 74% higher in mid-range treatments (~100–225g) at Day 89 (Figure S4; Tables S3 and S4). Phosphorus (as TDP) in treatment water was only measured once during the

experiment (Day 31). Similar to DOC at Day 10, TDP increased in both treatments with detritus loading and was 42% higher in the burned treatment at the highest-detritus level (400g) (Figure S5; Tables S3 and S4).

### 3.4 | Net primary productivity and respiration

Dissolved oxygen (as %  $O_2$ ) measurements showed consistent patterns among paired dawn measurements (separated by 24 h) in each time point (Figure S6). Percent  $O_2$  showed considerable change over time and treatments (Figure S7; model fits in Tables S5 and S6). Relative to unburned tanks, %  $O_2$  was consistently higher in mid-range burned treatments and lower in burned treatments receiving the highest plant material (400g) (Figure S6) (see *Supplemental Results*).

NPP (as  $\Delta$  %  $O_2$  from dawn to dusk) showed a significant non-linear relationship with plant biomass across all four time points. NPP was 30%–50% greater in burned relative to unburned tanks through Day 59 (Figure 4a; Tables S7 and S8). At Day 10, NPP exhibited an exponential decline with highest values in low-plant biomass treatments that also tended to be higher in burned tanks with low-plant biomass (Figure 4a; Figure S8A). By Day 31, NPP had stabilized across the plant-biomass gradient with a unimodal relationship

between NPP and biomass loading, and higher NPP in burned tanks ( $p=.007$ ). This pattern continued through Day 59, with an increasing unimodal relationship where highest NPP was observed in mid-range tanks (100–200g) and burned tanks ( $p=.012$ ) (Table S8). By Day 89, NPP in unburned tanks was flat across the plant biomass gradient ( $p=.327$ ) (Figure 4a), while NPP in burned tanks continued to show a unimodal relationship with plant biomass ( $p=.020$ ). NPP at Day 89 was 50%–70% lower in burned tanks receiving >250g plant material compared to unburned tanks.

Respiration (Resp, as  $\Delta$  %  $O_2$  from dusk to dawn) mirrored NPP and was greatest (most negative) in low-biomass treatments throughout the experiment. We observed significant non-linear associations between Resp and plant biomass at Day 10 that did not differ between treatments ( $p=.229$ ) (Figure 4b); however, by Day 31 Resp was offset by treatment-level intercepts, with an overall significant treatment effect driving a 50% increase in rates of Resp (more negative) in burned tanks ( $p=.019$ ) (Tables S7 and S8). Treatment-specific non-linear effects of plant addition on Resp were found for both burned and unburned treatments at Day 59 ( $p<.001$ ) and burned tanks alone at Day 89 ( $p=.004$ ). Resp rates were greater (more negative) by 20%–50% in mid-range burned tanks (~100–225g) at Day 59; while at Day 89, Resp was reduced in burned tanks (least negative change in  $O_2$ ), being on average 74% less in high-range treatments (300–400g) compared to unburned tanks.

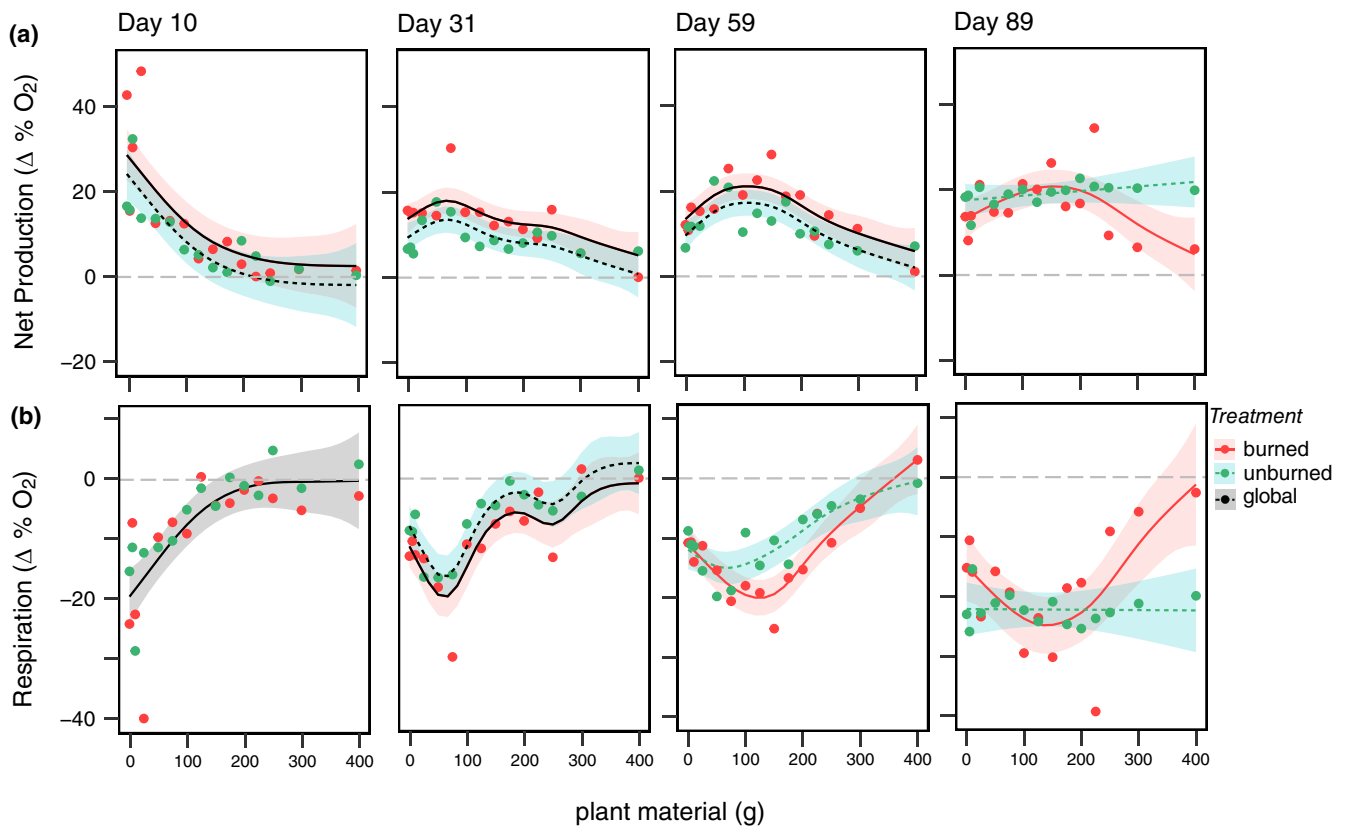


**FIGURE 4** (a) Net primary production and (b) respiration in treatments receiving burned and unburned plant material across four sampling periods. Lines represent best-fit generalized additive models with 95% confidence intervals. Black lines with gray confidence intervals indicate global smoothers across all data points; solid (burned) and dotted (unburned) black lines together represent treatment-level intercepts with global smoothers; colored lines indicate factor-smooths that vary between treatments.



### 3.5 | Plankton $^{15}\text{N}$ -labeling

We assessed trophic transfer using the integration of sage- $^{15}\text{N}$  into zooplankton biomass as a proxy for the assimilation of plant nutrition to consumers. Analysis of plant materials before being added to mesocosms showed mean ( $\pm\text{SE}$ ,  $n=11\text{--}12$ ) %N of plant material (stems and leaves, pooled across sage and willow) did not differ by treatment ( $p=.288$ ), being  $1.297\pm 0.126$  (burned) and  $1.178\pm 0.128$  (unburned). Subsequently, we used these %N values to estimate the total grams of plant-N added to each mesocosm (see plant and tissue specific %N in Figure 2).  $^{15}\text{N}$ -isotope labeling increased the  $\delta^{15}\text{N}$  isotope values of both burned-and-unburned sage ( $p<.001$ ), and burning treatment did not affect leaf  $\delta^{15}\text{N}$  values for sage ( $p=.423$ ) or willow ( $p=.485$ ) (see Supplemental Results; Figure S9; Table S9). Isotope mixing models showed a significant effect of plant material addition and burning on the trophic transfer (% sage- $^{15}\text{N}$ ) in plankton at Days 10 and 31 ( $p<.001$ ). Burned treatments showed an overall lower % sage- $^{15}\text{N}$  relative to unburned treatments (Figure 5; Tables S10 and S11), and no difference between plankton size fractions ( $<63\mu\text{m}$ ,  $>63\mu\text{m}$ ) was observed at either time point ( $p\geq.196$ ). At Days 10 and 31, both treatments showed a non-linear relationship between % sage- $^{15}\text{N}$  in plankton and detritus loading (as %N added) ( $p<.001$ ) (Table S11), where plankton % sage- $^{15}\text{N}$  increased with increased plant materials and %N following a saturating relationship. However, an asymptote for % sage- $^{15}\text{N}$  in the burned treatment occurred at lower plant addition levels in the burned treatment at Day 10 ( $\sim 300\text{g}$  of plant biomass). At Day 31, % sage- $^{15}\text{N}$  substantially declined in 400g burned treatment (Figure 5). Overall, burning progressively decreased trophic transfer and the incorporation of sage- $^{15}\text{N}$  into plankton in treatments receiving 50–400g of material at Day 10 (up to 20%) and  $\sim 75\text{--}125\text{g}$  and

$>300\text{g}$  at Day 31 (up to 28%) (Figure S10). These results show a greater integration of plant-derived nitrogen assimilated and transferred in the plankton food web in unburned treatments and a pronounced drop off in trophic transfer and greater autochthonous nutrition in burned treatments as detrital loading increased (Figure 5).

### 3.6 | Greenhouse gases

Prior to the addition of plant materials (Day 0),  $\text{CO}_2$  concentrations in tanks ranged from 20 to  $40\mu\text{M}$  (Figure 6a) equivalent to 530–1000ppm  $\text{CO}_2$  (ambient air 531ppm or  $20\mu\text{M}$   $\text{CO}_2$ ). After the addition of plant material,  $\text{CO}_2$  concentrations had increased to  $>300\mu\text{M}$   $\text{CO}_2$  ( $\sim 9000\text{ppm}$   $\text{CO}_2$ ) in the highest biomass tanks by Day 10 (Figure 6a), resulting in supersaturation and  $>1600\%$  excess  $\text{CO}_2$  (Figure S11). Significant relationships between  $\text{CO}_2$  concentrations and plant material were found for both burned and unburned treatments at all time points ( $p<.001$ ).  $\text{CO}_2$  concentrations were also consistently higher in the unburned relative to burned tanks in treatments receiving 100–325g plant material at Days 10, 31, and 59 (Figure S12; Tables S12 and S13).  $\text{CO}_2$  concentrations and percent excess were significantly higher in the burned treatments receiving 400g plant material at Day 31, and a similar trend was noted at Day 59 with a range of 140–250 $\mu\text{M}$   $\text{CO}_2$  and  $>500\%$  excess  $\text{CO}_2$  (Figure 6a; Figures S11 and S12).

In contrast to  $\text{CO}_2$ , the concentration of  $\text{CH}_4$  increased through time but was less impacted by treatments or plant biomass (Figure 6b). Treatment effects were most apparent at Day 10, where  $\text{CH}_4$  concentrations showed a non-linear relationship for unburned tanks only ( $p=.001$ ) and were higher in unburned tanks relative to burned tanks receiving  $>250\text{g}$  of plant material (Figure 6b; Figure S12). On

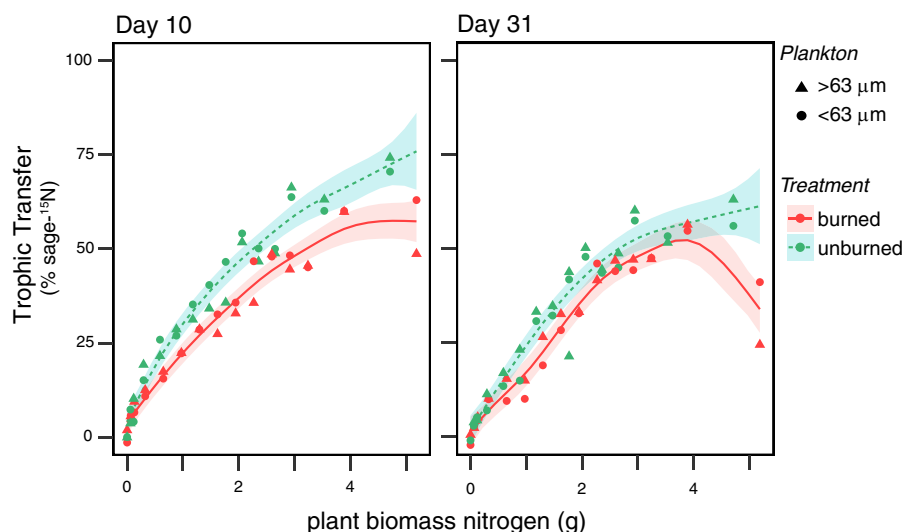


**FIGURE 5** Trophic transfer into particulate organic material ( $<63\mu\text{m}$ , circles) and zooplankton ( $>63\mu\text{m}$ , triangles) as the % sage- $^{15}\text{N}$  from a two-source mixing model as a metric for terrestrial subsidies at Days 10 and 31. Plant biomass nitrogen (x-axis) was calculated from the %N of total biomass of burned or unburned plant detritus added to tanks. Lines represent best-fit generalized additive models with 95% confidence intervals and factor-smooths that vary between treatments.

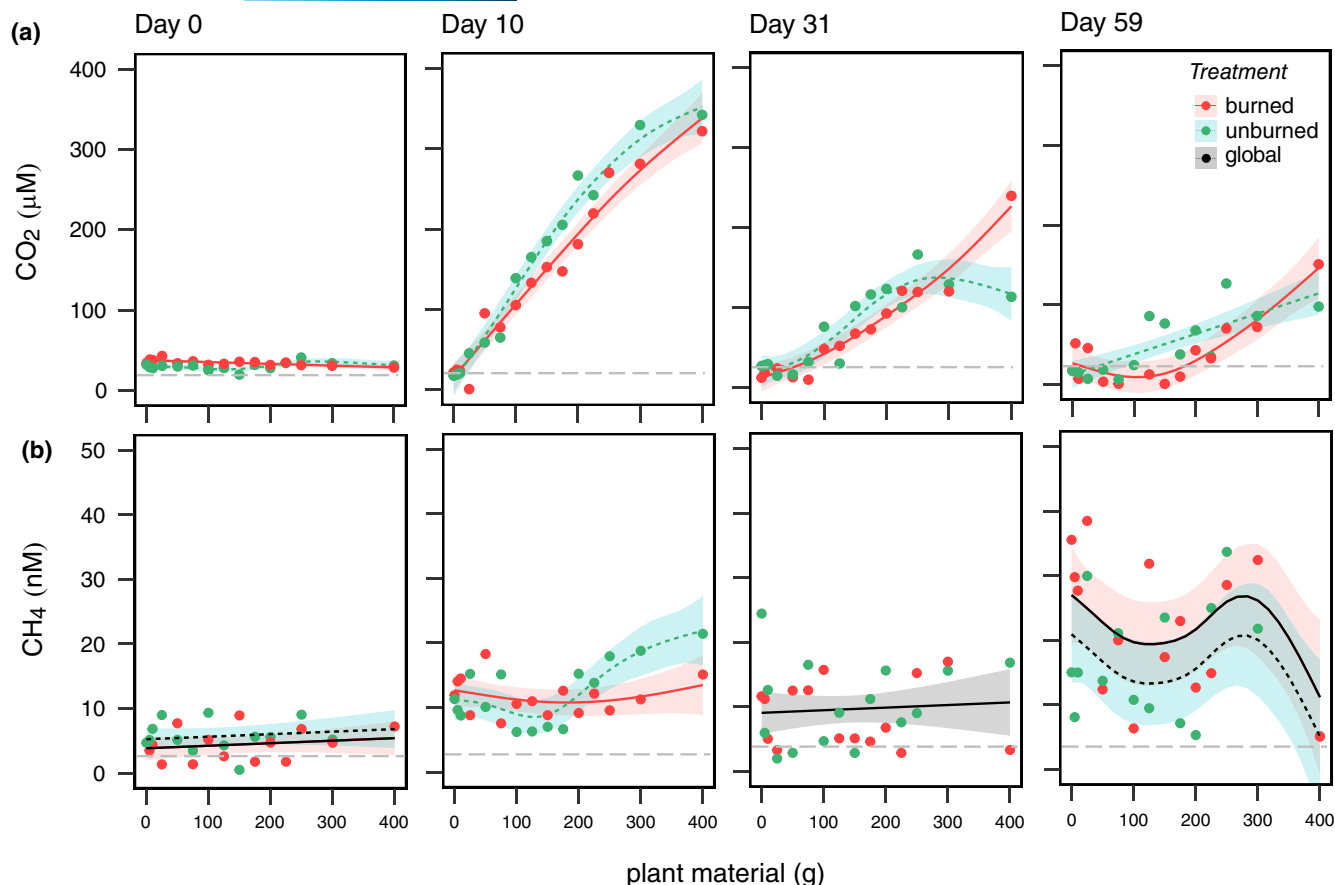


**FIGURE 6** Greenhouse gas concentration for (a) carbon dioxide ( $\text{CO}_2$ ) and (b) methane ( $\text{CH}_4$ ) in treatments receiving burned and unburned plant material at the beginning of the study (prior to adding materials [Day 0]) and across three experimental periods. Horizontal dashed lines (gray) indicate atmospheric gas concentrations at each sampling day. Lines represent best-fit generalized additive models with 95% confidence intervals. Black lines with gray confidence intervals indicate global smoothers across all data points; solid (burned) and dotted (unburned) black lines together represent treatment-level intercepts with global smoothers; colored lines indicate factor-smooths that vary between treatments.

Day 10,  $\text{CH}_4$  concentrations in burned tanks increased to  $\sim 12$  nM equivalent to 8 ppm  $\text{CH}_4$  (ambient air 2.3 nM or 1.9 ppm  $\text{CH}_4$ ) but were relatively stable across plant material loading. Conversely, unburned tanks  $\text{CH}_4$  concentration increased to  $>20$  nM (700% excess  $\text{CH}_4$ ), especially in tanks receiving  $>200$  g (Figure S11). No relationship between  $\text{CH}_4$  concentrations and plant-biomass or treatment was seen at Day 31 ( $p = .659$ ), although burned tanks tended to have higher  $\text{CH}_4$  concentrations and greater percent excess (25–40 nM  $\text{CH}_4$  and  $>600\%$  excess) in burned tanks at Day 59 (Figures S11 and S12; Table S13).

## 4 | DISCUSSION

Our results show that fire functionally alters the fate and impact of terrestrial organic subsidies in aquatic ecosystems and these impacts show non-linear dependencies on the quantity of terrestrial material introduced. The degradation of plant material in aquatic systems liberates nutrients and increases organic carbon (Blanchet et al., 2022) which can stimulate production under low

detrital-loading by supplying limiting nutrients (Figure 3; Figures S3 and S5) (Solomon et al., 2015). However, high detrital-loading causes light attenuation (Figure 1d) and can suppress aquatic primary production and respiration due to light absorption and oxygen depletion (Figure 4; Figure S6) (Solomon et al., 2015), ultimately reducing ecosystem stability by perturbing rates of nutrient turnover (Jones & Lennon, 2015). Our results show that, in addition to impacts on terrestrial ecosystems, fire also shifts the metabolism, trophic transfer, and greenhouse gas production of aquatic systems (Figures 5 and 6). Burning enhanced the impact of detrital loading on ecosystem production and respiration and dampened its effects on trophic transfer to plankton consumers. While burned treatments had greater NPP and autochthony, which led to lower  $\text{CO}_2$  concentrations compared to unburned treatments overall,  $\text{CO}_2$   $\mu\text{M}$  in burned treatments rose exponentially under highest plant detritus loading (400g). In addition, both  $\text{CO}_2$  and  $\text{CH}_4$  were supersaturated relative to the atmosphere through Day 59 (less so for  $\text{CO}_2$  in low-detritus burned tanks), commonly in excess of 1000% and 500% for  $\text{CO}_2$  and  $\text{CH}_4$ , respectively. These results show that increased terrestrial subsidies and wildfires may act to alter the greenhouse gas concentrations and

their emissions from lentic systems, increasing the export of these gases over short time scales (~60 days in the current experiment). Therefore, more frequent, and intense wildfires may alter the capacity of aquatic systems to store, transform, and exchange carbon with the atmosphere.

Increased terrestrial material and DOC drove unimodal effects on ecosystem metabolism as tanks transitioned from nutrient- to light-limitations (Jones & Lennon, 2015; Solomon et al., 2015). Burning magnified these patterns, with greater rates of system production and respiration at intermediate loading (Figure 4). At high detrital-loading (>250 g) burned tanks showed chronic destabilization with lower NPP, Resp, and DO persisting for ~90 days (Figure 4; Figure S6). Burning chemically transforms plant biomass (Butler et al., 2021) in ways that alter the feedbacks that link aquatic ecosystems to the metabolism, storage, and processing of terrestrial productivity. Wildfire impacts to aquatic ecosystems can persist for decades (Rodríguez-Cardona et al., 2020) but are especially dynamic in the first 5 years post-fire (Rust et al., 2018). Indeed, over the short period of our experiment (~90 days) we observed substantial temporal variability in water quality and productivity, suggesting a critical transition between terrestrial loading/DOC concentrations and the stimulatory effect of limiting nutrients on aquatic productivity (Stetler et al., 2021). In a companion study, we show that detrital loading and burning produce non-linear effects on the chemical composition of DOM in these tanks, with greater humification and specific ultraviolet absorbance (i.e., SUVA 254 nm, a proxy for aromaticity); however, humification decreased more rapidly in burned treatments compared to unburned (Spiegel et al., 2023). Therefore, greater NPP and lower DOC in the burned treatment may be a result of fire effects on the organic chemistry of the parent materials and the processing of DOM in aquatic ecosystems. However, it is notable that positive impacts of fire on liberating dissolved organic and inorganic nutrients (e.g., N, P, DOC, DOM) (Hampton et al., 2022) and stimulating water column production at low- and intermediate-loadings give way to tipping points where aquatic ecosystems are driven to dystrophic states under conditions of high terrestrial inputs. Fire also reduced both greenhouse gas concentrations and the transfer of detritus (plant-derived N) to higher trophic levels (Figures 5 and 6). Therefore, accounting for feedback between wildfire and aquatic productivity and CO<sub>2</sub> concentration from freshwater ecosystems may be critical for a complete accounting of the role of fire in the global carbon cycle (Lasslop et al., 2019; ; Liu, Zhou, et al., 2022; Pilla et al., 2022).

The impacts of fire and terrestrial subsidies in our mesocosm experiment significantly affected aquatic ecosystem function (metabolism, water chemistry, trophic transfer); however, these effects showed distinct temporal patterns related to time-since-disturbance (i.e., plant material introduction) and the amount of plant material added. For instance, terrestrial loading led to rapid, non-linear increases in DOC and CO<sub>2</sub> concentrations at Day 10 that reduced aquatic NPP and Resp (as well as %DO [Figure S6]) to near zero as detritus loading increased. The non-linear relationship between detritus loading and DOC concentration indicates that organic carbon

tended to be respired and subsequently fixed by primary producers at intermediate concentrations. Yet, DOC accumulated in the water column at the highest loading levels, attenuating light and reducing NPP, and contributing to rising CO<sub>2</sub> excess and its export to the atmosphere. Terrestrial-DOC (t-DOC) is the dominant form of terrestrial organic matter in lakes (Brett et al., 2012), however, <2% of t-DOC is transferred to zooplankton biomass relative to terrestrial particulate organic carbon (t-POC) (33%–73% in zooplankton) (Cole et al., 2006). Lake bacterioplankton actively assimilate low-molecular weight, labile DOC of algal and terrestrial origin (Guillemette et al., 2013), albeit algal-DOC is preferentially used in respiration and t-DOC in biosynthesis pathways (Guillemette et al., 2016). Nevertheless, the carbon transfer efficiency of algal- and terrestrial organic matter into plankton biomass are similar (0.2% and 0.4%, respectively) (Grosbois et al., 2020). Bacterial contributions to productivity and respiration have been shown to increase with DOC loading (Cole et al., 2006; Jones & Lennon, 2015) and in our study, elevated microbial respiration under increased detrital-loading contributed to hypoxia early in the experiment and persistent greenhouse gas export. This led to consistently lower DO concentrations in high-loading mesocosms (Figure S6) that reduced the efficiency of biological degradation of organic material.

A companion study (Spiegel et al., 2023) found that DOC decomposition in our experiment was strongly attributed to microbial activity than photodegradation, and that the highest rates of DOC decomposition occurred at intermediate concentrations. The saturating relationship between detrital loading and CO<sub>2</sub> concentrations also indicates that organic carbon was mineralized at slower rates at the highest concentrations where DOC accumulated, and DOC respiration was lower in burned treatments (Figure 6), possibly due to fire-effects on DOC composition such as increased aromaticity. Over time, a unimodal pattern relating terrestrial inputs with ecosystem metabolism emerged, and by Day 31 declines in DOC and CO<sub>2</sub> concentrations were matched with greater rates of NPP and Resp with distinct non-linear relationships across the plant-detritus gradient between the burned and unburned treatments. These patterns show that rising inputs of terrestrial detritus into aquatic systems—a global phenomenon known as “browning” (Blanchet et al., 2022)—produce non-linear feedbacks where both respiration and oxygenic primary production are stimulated by terrestrially derived nutrients and organic compounds at low and intermediate levels, but are suppressed by a combination of hypoxia, light limitation, and greater aromaticity at the highest levels (Jones & Lennon, 2015).

Burning altered the shapes of the non-linear functions between terrestrial loading and carbon dynamics and their evolution over time. Tanks receiving burned plant material had significantly higher NPP (on Days 10, 31, and 59) and Resp (on Days 31 and 59) than those with unburned material, and this effect was most pronounced at intermediate loading treatments. The greater stimulation of ecosystem metabolism—primarily NPP—in burned treatments may be a result of an increase in limiting nutrients (%N, %P, %K, %S, Zn ppm) (Figure 2) or greater consumption of terrestrial-DOM by heterotrophic bacteria in burned tanks

releasing inorganic substances that favor autochthonous nutrient pathways (Jones, 1992; Jones & Lennon, 2015). However, at high detrital-loading, dissolved phosphorus accumulated and this effect was accentuated by burning (Figure S6), indicating a reduction of energy transfer across trophic levels (Jones & Lennon, 2015). This effect may be due to a combination of (1) fire-induced changes in DOC chemistry (increased aromaticity) (Hampton et al., 2022; Spiegel et al., 2023), (2) plant polyphenols affecting enzyme activity (Hättenschwiler & Vitousek, 2000), (3) and/or changes to nutrient cycling between autotrophic and heterotrophic microorganisms (Cole et al., 1988).

Greenhouse gases also showed distinct fire effects later in the experiment, with burned tanks exhibiting both lower (intermediate detrital-loading) and higher (high detrital-loading) CO<sub>2</sub> than unburned tanks at Days 31 and 59. Lower CO<sub>2</sub> concentrations in the burned treatment at intermediate detrital-loading agrees with greater NPP in these tanks relative to the unburned tanks. CH<sub>4</sub> concentrations increased four-fold across time in all tanks and were higher in the burned treatment at the end of the experiment. Natural ponds and lakes account for 67% of CH<sub>4</sub> emissions from inland waters (Pilla et al., 2022), and the progressive rise in methane across our experiment may be the result of an increase in anaerobic methanogenesis localized within the detritus mesh bags as well as aerobic methanogenesis produced during bacterial photosynthesis (Perez-Coronel & Beman, 2022). The trend for higher CH<sub>4</sub> in the burned-detritus mesocosms at the end of the experiment, may likewise relate to greater autochthony and NPP in burned tanks also acting to stimulate bacterial methanogenesis. These results show that feedbacks between fire and warming may increase NPP and draw down CO<sub>2</sub> in lentic systems, which may favor CH<sub>4</sub> production. Taken together, these results show that the chemical transformation of terrestrial plant biomass by fire can lead to changes in the functioning of aquatic ecosystems, their metabolism, and the concentration of greenhouse gases, and these effects depend both on the loading of terrestrial subsidies, their quality, and time since disturbance.

High loading of plant detritus increased DOC and other humic compounds that limited primary production and resulted in greater reliance of heterotrophic zooplankton on terrestrial resources. Zooplankton can utilize terrestrial organic carbon (t-OC), although the benefits of t-OC for zooplankton nutrition and growth is context-dependent (Brett et al., 2009; Cole et al., 2011; Kelly et al., 2014). Relative to autochthonous nutrition, t-OC is low in nutritional quality due to high C:P and low unsaturated fatty acids (Brett et al., 2009). Phytoplankton-derived fatty acids are rapidly incorporated into zooplankton biomass reserves, supporting key ecological processes (i.e., overwintering, reproduction, trophic transfer) (Grosbois et al., 2017). In natural lakes increasing t-OC and allochthony were found to reduce zooplankton production (Kelly et al., 2014). Greater consumption of recalcitrant carbon and an inefficient microbial loop (Cole et al., 2002) may explain lower zooplankton production and rates of nutrient transfer across trophic levels where t-OC is high. We observed that % sage-<sup>15</sup>N in

two zooplankton size fractions increased with detrital-loading and was reduced in burned treatments; thus, burning reduced trophic transfer of plant-N to higher trophic levels (Figure 5). While mixing model values represent the relative contribution of sage as a terrestrial resource to plankton, they do not represent full accounting of terrestrial inputs due to the added contribution of willow (at natural isotope abundance). Plant-derived N incorporation in zooplankton depended on the interaction between detrital-loading and burning treatments. The saturating kinetics of this relationship show the assimilation of plant derived nitrogen to zooplankton increased proportionally as NPP decreased, supplying nutrients up to the highest loading levels where trophic transfer was markedly reduced. This effect was strongest in the burned treatments where zooplankton contained less sage-<sup>15</sup>N than in the unburned treatment. Greater utilization of algae/autochthonous versus plant detritus/allochthonous food sources was also observed in macroinvertebrates and fishes in post-fire (<5 years) streams, possibly due to fire reducing tree canopies and increasing light availability (Spencer et al., 2003). Therefore, fire may impact aquatic food webs by transforming the elemental composition of detritus and abiotic traits (i.e., terrestrial- and in-water shading, temperature; Barneche et al., 2021) important for ecosystem metabolism and trophic transfer. These effects can drive both short- and long-term changes in productivity, feeding behavior, and the transfer of energy in food webs.

We observed lower DOC (Figure 3) and higher NPP (Figure 4) in burned tanks to also coincide with a greater proportion of autochthonous nutrition and less plant-derived nutrition (using % sage-<sup>15</sup>N as a proxy) in zooplankton compared to unburned treatments. In a companion study (Spiegel et al., 2023), decomposition (% mass loss) of burned sage was twofold greater than burned willow after ~90 days, but the decomposition of burned and unburned sage was largely equivalent across the detrital-loading gradient. Therefore, lower % sage-<sup>15</sup>N in burned treatments overall and the marked decline at high detrital-loading, is likely not driven by difference in rates of <sup>15</sup>N release from burned/unburned sage, but instead changes in dissolved compounds, their lability, and composition (e.g., aromaticity) (Hampton et al., 2022; Rodríguez-Cardona et al., 2020). Overall, this pattern indicates that the effects of fire on biogeochemistry, microbial communities, and ecosystem metabolism are intimately related, and fire affects the trophic transfer of detrital nutrients to top consumers through alternate energy pathways.

While our study was designed to specifically test the influence of fire on terrestrial subsidies (in the form of plant detritus), it is important to recognize that wildfire effects on aquatic systems can persist for many years (Santos et al., 2019) and be felt locally as well as thousands of miles away through atmospheric and hydrological transport (Tang et al., 2021; Ward et al., 2022). Wildfires alter many constitutive ecosystem properties (e.g., soil chemistry, plant communities, erosion/deposition, detritus quality and quantity) and are capable of crossing ecosystem boundaries. Therefore, more long-term field studies and manipulative experiments are both needed to better understand the pathways through which wildfires will transform terrestrial and aquatic ecosystem structure and function.

Our study suggests that a complete accounting of the impact of browning and wildfire on the global carbon cycle must include feedbacks to the functioning of aquatic ecosystems. Inland waters transform and store carbon in their sediments at rates comparable to the global oceans (Ward et al., 2017). Lakes and ponds are significant sources of carbon to the atmosphere due to respiration of organic material of terrestrial origin (Pilla et al., 2022). Growing inputs of plant detritus into lakes and rivers and increased frequency and severity of wildfires (Pausas & Keeley, 2021) are two symptoms of recent global climate change and human activities. Our results indicate that these two forces may interact in ways that affect the capacity of aquatic systems to store, process and emit carbon. Accurate forecasts of ongoing climate change, therefore, require integrative models that incorporate feedbacks within and between aquatic and terrestrial ecosystems and consideration of how changing ignition patterns and wildfires will modify the global carbon cycle.

### AUTHOR CONTRIBUTIONS

**Christopher B. Wall:** Conceptualization; data curation; formal analysis; investigation; methodology; project administration; software; supervision; validation; visualization; writing – original draft; writing – review and editing. **Cody J. Spiegel:** Conceptualization; data curation; formal analysis; investigation; methodology; software; validation; visualization; writing – original draft; writing – review and editing. **Evelyn M. Diaz:** Investigation; methodology; writing – review and editing. **Cindy H. Tran:** Investigation; methodology; writing – review and editing. **Alexia Fabiani:** Investigation; methodology. **Taryn Y. Broe:** Investigation; methodology; writing – review and editing. **Elisabet Perez-Coronel:** Formal analysis; investigation; methodology; validation; visualization; writing – original draft; writing – review and editing. **Sara L. Jackrel:** Conceptualization; data curation; formal analysis; funding acquisition; investigation; methodology; validation; writing – original draft; writing – review and editing. **Natalie Mladenov:** Conceptualization; formal analysis; funding acquisition; investigation; methodology; resources; writing – original draft. **Celia C. Symons:** Conceptualization; investigation; writing – original draft; writing – review and editing. **Jonathan B. Shurin:** Conceptualization; funding acquisition; investigation; project administration; resources; supervision; visualization; writing – original draft; writing – review and editing.

### ACKNOWLEDGEMENTS

We thank Tobias Bautista, Kirby Inocente, Tristie Le, Ariana Brisco-Schoefield, Keyshawn Ford, Wenbo Ding, and Ryan Koch for their assistance in data collection and processing; Dr. Eric Schmelz for logistical support; and Emily Schick and the University of California-Davis Stable Isotope Facility for isotope and greenhouse gas analyses. This project was funded by support from the National Science Foundation (award number 2018058).

### CONFLICT OF INTEREST STATEMENT

The authors declare no conflicts of interest.

### DATA AVAILABILITY STATEMENT

All data and scripts are available at Github (<http://www.github.com/cbwall/Pyromania>) and are archived at Zenodo (Wall & Spiegel, 2023).

### ORCID

Christopher B. Wall  <https://orcid.org/0000-0002-7164-3201>  
 Cody J. Spiegel  <https://orcid.org/0000-0001-5889-0841>  
 Cindy H. Tran  <https://orcid.org/0000-0002-3352-5239>  
 Taryn Y. Broe  <https://orcid.org/0009-0007-8776-2890>  
 Elisabet Perez-Coronel  <https://orcid.org/0000-0003-2496-3840>  
 Natalie Mladenov  <https://orcid.org/0000-0002-6984-2180>  
 Celia C. Symons  <https://orcid.org/0000-0003-4120-0327>  
 Jonathan B. Shurin  <https://orcid.org/0000-0001-7870-1972>

### REFERENCES

- Ball, G., Regier, P., González-Pinzón, R., Reale, J., & Van Horn, D. (2021). Wildfires increasingly impact western US fluvial networks. *Nature Communications*, 12(1), 2484. <https://doi.org/10.1038/s41467-021-22747-3>
- Barneche, D. R., Hulatt, C. J., Dossena, M., Padfield, D., Woodward, G., Trimmer, M., & Yvon-Durocher, G. (2021). Warming impairs trophic transfer efficiency in a long-term field experiment. *Nature*, 592(7852), 76–79. <https://doi.org/10.1038/s41586-021-03352-2>
- Bixby, R. J., Cooper, S. D., Gresswell, R. E., Brown, L. E., Dahm, C. N., & Dwire, K. A. (2015). Fire effects on aquatic ecosystems: An assessment of the current state of the science. *Freshwater Science*, 34(4), 1340–1350. <https://doi.org/10.1086/684073>
- Bladon, K. D., Silins, U., Wagner, M. J., Stone, M., Emelko, M. B., Mendoza, C. A., Devito, K. J., & Boon, S. (2008). Wildfire impacts on nitrogen concentration and production from headwater streams in southern Alberta's Rocky Mountains. *Canadian Journal of Forest Research. Journal Canadien de La Recherche Forestiere*, 38(9), 2359–2371. <https://doi.org/10.1139/x08-071>
- Blanchet, C. C., Arzel, C., Davranche, A., Kahilainen, K. K., Secondi, J., Taipale, S., Lindberg, H., Loehr, J., Manninen-Johansen, S., Sundell, J., Maanan, M., & Nummi, P. (2022). Ecology and extent of freshwater browning—What we know and what should be studied next in the context of global change. *The Science of the Total Environment*, 812, 152420. <https://doi.org/10.1016/j.scitotenv.2021.152420>
- Bowman, D. M. J. S., Balch, J. K., Artaxo, P., Bond, W. J., Carlson, J. M., Cochrane, M. A., D'Antonio, C. M., Defries, R. S., Doyle, J. C., Harrison, S. P., Johnston, F. H., Keeley, J. E., Krawchuk, M. A., Kull, C. A., Marston, J. B., Moritz, M. A., Prentice, I. C., Roos, C. I., Scott, A. C., ... Pyne, S. J. (2009). Fire in the earth system. *Science*, 324(5926), 481–484. <https://doi.org/10.1126/science.1163886>
- Brett, M. T., Arhonditsis, G. B., Chandra, S., & Kainz, M. J. (2012). Mass flux calculations show strong allochthonous support of freshwater zooplankton production is unlikely. *PLoS ONE*, 7(6), e39508. <https://doi.org/10.1371/journal.pone.0039508>
- Brett, M. T., Kainz, M. J., Taipale, S. J., & Seshan, H. (2009). Phytoplankton, not allochthonous carbon, sustains herbivorous zooplankton production. *Proceedings of the National Academy of Sciences of the United States of America*, 106(50), 21197–21201. <https://doi.org/10.1073/pnas.0904129106>
- Butler, O. M., Elser, J. J., Lewis, T., Maunsell, S. C., Rezaei Rashti, M., & Chen, C. (2020). The multi-element stoichiometry of wet eucalypt forest is transformed by recent, frequent fire. *Plant and Soil*, 447(1), 447–461. <https://doi.org/10.1007/s11104-019-04397-z>
- Butler, O. M., Lewis, T., Maunsell, S. C., Rezaei Rashti, M., Elser, J. J., Mackey, B., & Chen, C. (2021). The stoichiometric

- signature of high-frequency fire in forest floor food webs. *Ecological Monographs*, 91, e01477. <https://doi.org/10.1002/ecm.1477>
- Carignan, R., D'Arcy, P., & Lamontagne, S. (2000). Comparative impacts of fire and forest harvesting on water quality in Boreal Shield lakes. *Canadian Journal of Fisheries and Aquatic Sciences*, 57(S2), 105–117.
- Cole, J. J., Carpenter, S. R., Kitchell, J., Pace, M. L., Solomon, C. T., & Weidel, B. (2011). Strong evidence for terrestrial support of zooplankton in small lakes based on stable isotopes of carbon, nitrogen, and hydrogen. *Proceedings of the National Academy of Sciences of the United States of America*, 108(5), 1975–1980. <https://doi.org/10.1073/pnas.1012807108>
- Cole, J. J., Carpenter, S. R., Kitchell, J. F., & Pace, M. L. (2002). Pathways of organic carbon utilization in small lakes: Results from a whole-lake <sup>13</sup>C addition and coupled model. *Limnology and Oceanography*, 47(6), 1664–1675. <https://doi.org/10.4319/lo.2002.47.6.1664>
- Cole, J. J., Carpenter, S. R., Pace, M. L., Van de Bogert, M. C., Kitchell, J. L., & Hodgson, J. R. (2006). Differential support of lake food webs by three types of terrestrial organic carbon. *Ecology Letters*, 9(5), 558–568. <https://doi.org/10.1111/j.1461-0248.2006.00898.x>
- Cole, J. J., Findlay, S., & Pace, M. L. (1988). Bacterial production in fresh and saltwater ecosystems: A cross-system overview. *Marine Ecology Progress Series*, 43, 1–10. <https://doi.org/10.3354/meps043001>
- Coretta, S., van Rij, J., & Wieling, M. (2022). *Tidymv: tidy model visualisation for generalised additive models*. R package version. <https://cran.r-project.org/web/packages/tidymv/index.html>
- Cottingham, K. L., Lennon, J. T., & Brown, B. L. (2005). Knowing when to draw the line: Designing more informative ecological experiments. *Frontiers in Ecology and the Environment*, 3(3), 145–152. [https://doi.org/10.1890/1540-9295\(2005\)003\[0145:kwtdt\]2.0.co;2](https://doi.org/10.1890/1540-9295(2005)003[0145:kwtdt]2.0.co;2)
- Dahm, C. N., Candelaria-Ley, R. I., Reale, C. S., Reale, J. K., & Van Horn, D. J. (2015). Extreme water quality degradation following a catastrophic forest fire. *Freshwater Biology*, 60(12), 2584–2599. <https://doi.org/10.1111/fwb.12548>
- Diemer, L. A., McDowell, W. H., Wymore, A. S., & Prokushkin, A. S. (2015). Nutrient uptake along a fire gradient in boreal streams of Central Siberia. *Freshwater Science*, 34(4), 1443–1456. <https://doi.org/10.1086/683481>
- Fei, S., Morin, R. S., Oswalt, C. M., & Liebhold, A. M. (2019). Biomass losses resulting from insect and disease invasions in US forests. *Proceedings of the National Academy of Sciences of the United States of America*, 116(35), 17371–17376. <https://doi.org/10.1073/pnas.1820601116>
- Fox, J., & Weisberg, S. (2019). *An R companion to applied regression* (3rd ed.). Sage. <https://socialsciences.mcmaster.ca/jfox/Books/Companion/>
- Grosbois, G., Mariash, H., Schneider, T., & Rautio, M. (2017). Under-ice availability of phytoplankton lipids is key to freshwater zooplankton winter survival. *Scientific Reports*, 7(1), 11543. <https://doi.org/10.1038/s41598-017-10956-0>
- Grosbois, G., Vachon, D., Del Giorgio, P. A., & Rautio, M. (2020). Efficiency of crustacean zooplankton in transferring allochthonous carbon in a boreal lake. *Ecology*, 101(6), e03013. <https://doi.org/10.1002/ecy.3013>
- Guillemette, F., Leigh McCallister, S., & Del Giorgio, P. A. (2016). Selective consumption and metabolic allocation of terrestrial and algal carbon determine allochthony in lake bacteria. *The ISME Journal*, 10(6), 1373–1382. <https://doi.org/10.1038/ismej.2015.215>
- Guillemette, F., McCallister, S. L., & del Giorgio, P. A. (2013). Differentiating the degradation dynamics of algal and terrestrial carbon within complex natural dissolved organic carbon in temperate lakes. *Journal of Geophysical Research. Biogeosciences*, 118(3), 963–973. <https://doi.org/10.1002/jgrg.20077>
- Hampton, T. B., Lin, S., & Basu, N. B. (2022). Forest fire effects on stream water quality at continental scales: A meta-analysis. *Environmental Research Letters*, 17(6), 064003. <https://doi.org/10.1088/1748-9326/ac6a6c>
- Hättenschwiler, S., & Vitousek, P. M. (2000). The role of polyphenols in terrestrial ecosystem nutrient cycling. *Trends in Ecology & Evolution*, 15(6), 238–243. [https://doi.org/10.1016/s0169-5347\(00\)01861-9](https://doi.org/10.1016/s0169-5347(00)01861-9)
- Hicke, J. A., Allen, C. D., Desai, A. R., Dietze, M. C., Hall, R. J., Ted Hogg, E. H., Kashian, D. M., Moore, D., Raffa, K. F., Sturrock, R. N., & Vogelmann, J. (2012). Effects of biotic disturbances on forest carbon cycling in the United States and Canada. *Global Change Biology*, 18(1), 7–34. <https://doi.org/10.1111/j.1365-2486.2011.02543.x>
- Isidorova, A., Bravo, A. G., Riise, G., Bouchet, S., Björn, E., & Sobek, S. (2016). The effect of lake browning and respiration mode on the burial and fate of carbon and mercury in the sediment of two boreal lakes. *Journal of Geophysical Research. Biogeosciences*, 121(1), 233–245. <https://doi.org/10.1002/2015jg003086>
- Jones, M. W., Abatzoglou, J. T., Veraverbeke, S., Andela, N., Lasslop, G., Forkel, M., Smith, A. J. P., Burton, C., Betts, R. A., van der Werf, G. R., Sitch, S., Canadell, J. G., Santín, C., Kolden, C., Doerr, S. H., & Le Quéré, C. (2022). Global and regional trends and drivers of fire under climate change. *Reviews of Geophysics*, 60(3), e2020RG000726. <https://doi.org/10.1029/2020rg000726>
- Jones, R. I. (1992). The influence of humic substances on lacustrine planktonic food chains. *Hydrobiologia*, 229(1), 73–91. <https://doi.org/10.1007/bf00006992>
- Jones, S. E., & Lennon, J. T. (2015). A test of the subsidy–stability hypothesis: The effects of terrestrial carbon in aquatic ecosystems. *Ecology*, 96(6), 1550–1560. <https://doi.org/10.1890/14-1783.1>
- Karlsson, J., Bergström, A.-K., Byström, P., Gudasz, C., Rodríguez, P., & Hein, C. (2015). Terrestrial organic matter input suppresses biomass production in lake ecosystems. *Ecology*, 96(11), 2870–2876. <https://doi.org/10.1890/15-0515.1>
- Karpowicz, M., Feniova, I., Gladyshev, M. I., Ejsmont-Karabin, J., Górniak, A., Sushchik, N. N., Anishchenko, O. V., & Dzialowski, A. R. (2021). Transfer efficiency of carbon, nutrients, and polyunsaturated fatty acids in planktonic food webs under different environmental conditions. *Ecology and Evolution*, 11(12), 8201–8214. <https://doi.org/10.1002/ece3.7651>
- Kelly, P. T., Solomon, C. T., Weidel, B. C., & Jones, S. E. (2014). Terrestrial carbon is a resource, but not a subsidy, for lake zooplankton. *Ecology*, 95(5), 1236–1242. <https://doi.org/10.1890/13-1586.1>
- Kocic, J., Wallin, M. B., Chmiel, H. E., Denfeld, B. A., & Sobek, S. (2015). Carbon dioxide evasion from headwater systems strongly contributes to the total export of carbon from a small boreal lake catchment. *Journal of Geophysical Research. Biogeosciences*, 120(1), 13–28. <https://doi.org/10.1002/2014jg002706>
- Koschorreck, M., Prairie, Y. T., Kim, J., & Marcé, R. (2021). Technical note: CO<sub>2</sub> is not like CH<sub>4</sub>—Limits of and corrections to the headspace method to analyse pCO<sub>2</sub> in fresh water. *Biogeosciences*, 18(5), 1619–1627. <https://doi.org/10.5194/bg-18-1619-2021>
- Kreyling, J., Schweiger, A. H., Bahn, M., Ineson, P., Migliavacca, M., Morel-Journel, T., Christiansen, J. R., Schtickzelle, N., & Larsen, K. S. (2018). To replicate, or not to replicate - that is the question: How to tackle nonlinear responses in ecological experiments. *Ecology Letters*, 21(11), 1629–1638. <https://doi.org/10.1111/ele.13134>
- Lafage, D., Bergman, E., Eckstein, R. L., Österling, E. M., Sadler, J. P., & Piccolo, J. J. (2019). Local and landscape drivers of aquatic-to-terrestrial subsidies in riparian ecosystems: A worldwide meta-analysis. *Ecosphere*, 10(4), e02697. <https://doi.org/10.1002/ecs2.2697>
- Larsen, I. J., MacDonald, L. H., Brown, E., Rough, D., Welsh, M. J., Pietraszek, J. H., Libohova, Z., Dios Benavides-Solorio, J., & Schaffrath, K. (2009). Causes of post-fire runoff and erosion: Water repellency, cover, or soil sealing? *Soil Science Society of America Journal*, 73(4), 1393–1407. <https://doi.org/10.2136/sssaj2007.0432>

- Lasslop, G., Coppola, A. I., Voulgarakis, A., Yue, C., & Veraverbeke, S. (2019). Influence of fire on the carbon cycle and climate. *Current Climate Change Reports*, 5(2), 112–123. <https://doi.org/10.1007/s40641-019-00128-9>
- Lennon, J. T. (2004). Experimental evidence that terrestrial carbon subsidies increase CO<sub>2</sub> flux from lake ecosystems. *Oecologia*, 138(4), 584–591. <http://www.jstor.org/stable/40005540>
- Lennon, J. T., & Pfaff, L. E. (2005). Source and supply of terrestrial organic matter affects aquatic microbial metabolism. *Aquatic Microbial Ecology: International Journal*, 39, 107–119. <https://doi.org/10.3354/ame039107>
- Lewis, J., Rhodes, J. J., & Bradley, C. (2019). Turbidity responses from timber harvesting, wildfire, and post-fire logging in the Battle Creek Watershed, Northern California. *Environmental Management*, 63(3), 416–432. <https://doi.org/10.1007/s00267-018-1036-3>
- Liu, D., Zhou, C., Keesing, J. K., Serrano, O., Werner, A., Fang, Y., Chen, Y., Masque, P., Kinloch, J., Sadekov, A., & Du, Y. (2022). Wildfires enhance phytoplankton production in tropical oceans. *Nature Communications*, 13(1), 1348. <https://doi.org/10.1038/s41467-022-29013-0>
- Liu, Y., Stanturf, J., & Goodrick, S. (2010). Trends in global wildfire potential in a changing climate. *Forest Ecology and Management*, 259(4), 685–697. <https://doi.org/10.1016/j.foreco.2009.09.002>
- Liu, Z., Deng, Z., Davis, S. J., Giron, C., & Ciais, P. (2022). Monitoring global carbon emissions in 2021. *Nature Reviews Earth and Environment*, 3(4), 217–219. <https://doi.org/10.1038/s43017-022-00285-w>
- McCullough, I. M., Cheruvelil, K. S., Lapiere, J.-F., Lottig, N. R., Moritz, M. A., Stachelek, J., & Soranno, P. A. (2019). Do lakes feel the burn? Ecological consequences of increasing exposure of lakes to fire in the continental United States. *Global Change Biology*, 25(9), 2841–2854. <https://doi.org/10.1111/gcb.14732>
- McLauchlan, K. K., Higuera, P. E., Miesel, J., Rogers, B. M., Schweitzer, J., Shuman, J. K., Tepley, A. J., Varner, J. M., Veblen, T. T., Adalsteinsson, S. A., Balch, J. K., Baker, P., Batllori, E., Bigio, E., Brando, P., Cattau, M., Chipman, M. L., Coen, J., Crandall, R., ... Watts, A. C. (2020). Fire as a fundamental ecological process: Research advances and frontiers. *The Journal of Ecology*, 108(5), 2047–2069. <https://doi.org/10.1111/1365-2745.13403>
- Millero, F. J. (1979). The thermodynamics of the carbonate system in seawater. *Geochimica et Cosmochimica Acta*, 43(10), 1651–1661. [https://doi.org/10.1016/0016-7037\(79\)90184-4](https://doi.org/10.1016/0016-7037(79)90184-4)
- Millero, F. J. (2010). Carbonate constants for estuarine waters. *Marine and Freshwater Research*, 61(2), 139–142. <https://doi.org/10.1071/MF09254>
- Minshall, G. W., Brock, J. T., Andrews, D. A., & Robinson, C. T. (2001). Water quality, substratum and biotic responses of five Central Idaho (USA) streams during the first year following the Mortar Creek fire. *International Journal of Wildland Fire*, 10(2), 185. <https://doi.org/10.1071/wf01017>
- Natali, S. M., Holdren, J. P., Rogers, B. M., Treharne, R., Duffy, P. B., Pomeroy, R., & MacDonald, E. (2021). Permafrost carbon feedbacks threaten global climate goals. *Proceedings of the National Academy of Sciences of the United States of America*, 118(21), e2100163118. <https://doi.org/10.1073/pnas.2100163118>
- Obernosterer, I., & Benner, R. (2004). Competition between biological and photochemical processes in the mineralization of dissolved organic carbon. *Limnology and Oceanography*, 49(1), 117–124. <https://doi.org/10.4319/lo.2004.49.1.0117>
- Paul, M. J., LeDuc, S. D., Lassiter, M. G., Moorhead, L. C., Noyes, P. D., & Leibowitz, S. G. (2022). Wildfire induces changes in receiving waters: A review with considerations for water quality management. *Water Resources Research*, 58(9), 1–28. <https://doi.org/10.1029/2021wr030699>
- Pausas, J. G., & Keeley, J. E. (2021). Wildfires and global change. *Frontiers in Ecology and the Environment*, 19(7), 387–395. <https://doi.org/10.1002/fee.2359>
- Pedersen, E. J., Miller, D. L., Simpson, G. L., & Ross, N. (2019). Hierarchical generalized additive models in ecology: An introduction with mgcv. *PeerJ*, 7, e6876. <https://doi.org/10.7717/peerj.6876>
- Pellegrini, A. F. A., Harden, J., Georgiou, K., Hemes, K. S., Malhotra, A., Nolan, C. J., & Jackson, R. B. (2021). Fire effects on the persistence of soil organic matter and long-term carbon storage. *Nature Geoscience*, 15(1), 5–13. <https://doi.org/10.1038/s41561-021-00867-1>
- Perez-Coronel, E., Hart, S. C., & Beman, J. M. (2021). Methane dynamics of high-elevation lakes in the Sierra Nevada California: The role of elevation, temperature, and inorganic nutrients. *Inland Waters*, 11(3), 267–277. <https://doi.org/10.1080/20442041.2021.1903287>
- Perez-Coronel, E., & Beman, J. M. (2022). Multiple sources of aerobic methane production in aquatic ecosystems include bacterial photosynthesis. *Nature Communications*, 13(1), 6454. <https://doi.org/10.1038/s41467-022-34105-y>
- Pilla, R. M., Griffiths, N. A., Gu, L., Kao, S.-C., McManamay, R., Ricciuto, D. M., & Shi, X. (2022). Anthropogenically driven climate and landscape change effects on inland water carbon dynamics: What have we learned and where are we going? *Global Change Biology*, 28(19), 5601–5629. <https://doi.org/10.1111/gcb.16324>
- Post, D. M. (2002). Using stable isotopes to estimate trophic position: Models, methods, and assumptions. *Ecology*, 83(3), 703–718. <https://doi.org/10.2307/3071875>
- R Core Team. (2022). R: A language and environment for statistical computing. R Foundation for Statistical Computing. <https://www.R-project.org/>
- Ramberg, L., Lindholm, M., Hessen, D. O., Murray-Hudson, M., Bonyongo, C., Heintz, M., Masamba, W., VanderPost, C., & Wolski, P. (2010). Aquatic ecosystem responses to fire and flood size in the Okavango Delta: Observations from the seasonal floodplains. *Wetlands Ecology and Management*, 18(5), 587–595. <https://doi.org/10.1007/s11273-010-9195-x>
- Rodríguez-Cardona, B. M., Coble, A. A., Wymore, A. S., Kolosov, R., Podgorski, D. C., Zito, P., Spencer, R. G. M., Prokushkin, A. S., & McDowell, W. H. (2020). Wildfires lead to decreased carbon and increased nitrogen concentrations in upland arctic streams. *Scientific Reports*, 10(1), 8722. <https://doi.org/10.1038/s41598-020-65520-0>
- Rodríguez-Lozano, P., Rieradevall, M., Rau, M. A., & Prat, N. (2015). Long-term consequences of a wildfire for leaf-litter breakdown in a Mediterranean stream. *Freshwater Science*, 34(4), 1482–1493. <https://doi.org/10.1086/683432>
- Rust, A. J., Hogue, T. S., Saxe, S., & McCray, J. (2018). Post-fire water-quality response in the western United States. *International Journal of Wildland Fire*, 27(3), 203–216. <https://doi.org/10.1071/WF17115>
- Santos, F., Wymore, A. S., Jackson, B. K., Sullivan, S. M. P., McDowell, W. H., & Berhe, A. A. (2019). Fire severity, time since fire, and site-level characteristics influence streamwater chemistry at baseflow conditions in catchments of the Sierra Nevada, California, USA. *Fire Ecology*, 15(1), 1–15. <https://doi.org/10.1186/s42408-018-0022-8>
- Simpson, G. L. (2022). *gratia: Graceful "ggplot"-based graphics and other functions for GAMs fitted using "mgcv"*. R Package Version 0.7.3. <https://gavinsimpson.github.io/gratia/>
- Sobek, S., Algesten, G., Bergström, A.-K., Jansson, M., & Tranvik, L. J. (2003). The catchment and climate regulation of pCO<sub>2</sub> in boreal lakes. *Global Change Biology*, 9(4), 630–641. <https://doi.org/10.1046/j.1365-2486.2003.00619.x>
- Solomon, C. T., Jones, S. E., Weidel, B. C., Buffam, I., Fork, M. L., Karlsson, J., Larsen, S., Lennon, J. T., Read, J. S., Sadro, S., & Saros, J. E. (2015). Ecosystem consequences of changing inputs of terrestrial dissolved organic matter to lakes: Current knowledge and future challenges. *Ecosystems*, 18(3), 376–389. <https://doi.org/10.1007/s10021-015-9848-y>
- Spencer, C. N., Gabel, K. O., & Hauer, F. R. (2003). Wildfire effects on stream food webs and nutrient dynamics in Glacier National Park,

- USA. *Forest Ecology and Management*, 178(1), 141–153. [https://doi.org/10.1016/S0378-1127\(03\)00058-6](https://doi.org/10.1016/S0378-1127(03)00058-6)
- Spiegel, C. J., Mladenov, N., Wall, C. B., Hollman, K., Tran, C. H., Symons, C. C., & Shurin, J. B. (2023). Life after a fiery death: Fire and plant biomass loading affect dissolved organic matter in experimental ponds. *Global Change Biology*, <https://doi.org/10.1111/gcb.17061>
- Stetler, J. T., Knoll, L. B., Driscoll, C. T., & Rose, K. C. (2021). Lake browning generates a spatiotemporal mismatch between dissolved organic carbon and limiting nutrients. *Limnology and Oceanography Letters*, 6(4), 182–191. <https://doi.org/10.1002/lol2.10194>
- Tang, W., Llort, J., Weis, J., Perron, M. M. G., Basart, S., Li, Z., Sathyendranath, S., Jackson, T., Sanz Rodriguez, E., Proemse, B. C., Bowie, A. R., Schallenberg, C., Strutton, P. G., Matear, R., & Cassar, N. (2021). Widespread phytoplankton blooms triggered by 2019–2020 Australian wildfires. *Nature*, 597(7876), 370–375. <https://doi.org/10.1038/s41586-021-03805-8>
- Wall, C. B., & Spiegel, C. J. (2023). cbwall/Pyromania: pub.ver (v.1.2). *Zenodo*, <https://doi.org/10.5281/zenodo.10045536>
- Ward, M., Southwell, D., Gallagher, R. V., Raadik, T. A., Whiterod, N. S., Lintermans, M., Sheridan, G., Nyman, P., Suárez-Castro, A. F., Marsh, J., Woinarski, J., & Legge, S. (2022). Modelling the spatial extent of post-fire sedimentation threat to estimate the impacts of fire on waterways and aquatic species. *Diversity and Distributions*, 28(11), 2429–2442. <https://doi.org/10.1111/ddi.13640>
- Ward, N. D., Bianchi, T. S., Medeiros, P. M., Seidel, M., Richey, J. E., Keil, R. G., & Sawakuchi, H. O. (2017). Where carbon goes when water flows: Carbon cycling across the aquatic continuum. *Frontiers in Marine Science*, 4. <https://doi.org/10.3389/fmars.2017.00007>
- Weiss, R. F. (1974). Carbon dioxide in water and seawater: The solubility of a non-ideal gas. *Marine Chemistry*, 2(3), 203–215. [https://doi.org/10.1016/0304-4203\(74\)90015-2](https://doi.org/10.1016/0304-4203(74)90015-2)
- Whitney, J. E., Gido, K. B., Pilger, T. J., Propst, D. L., & Turner, T. F. (2015). Consecutive wildfires affect stream biota in cold- and warmwater dryland river networks. *Freshwater Science*, 34(4), 1510–1526. <https://doi.org/10.1086/683391>
- Wood, S. N. (2011). Fast stable restricted maximum likelihood and marginal likelihood estimation of semiparametric generalized linear models. *Journal of the Royal Statistical Society. Series B, Statistical Methodology*, 73(1), 3–36. <https://doi.org/10.1111/j.1467-9868.2010.00749.x>
- Yamamoto, S., Alcauskas, J. B., & Crozier, T. E. (1976). Solubility of methane in distilled water and seawater. *Journal of Chemical and Engineering Data*, 21(1), 78–80. <https://doi.org/10.1021/je60068a029>
- Zheng, B., Ciais, P., Chevallier, F., Chuvieco, E., Chen, Y., & Yang, H. (2021). Increasing forest fire emissions despite the decline in global burned area. *Science Advances*, 7(39), eabh2646. <https://doi.org/10.1126/sciadv.abh2646>

## SUPPORTING INFORMATION

Additional supporting information can be found online in the Supporting Information section at the end of this article.

**How to cite this article:** Wall, C. B., Spiegel, C. J., Diaz, E. M., Tran, C. H., Fabiani, A., Broe, T. Y., Perez-Coronel, E., Jackrel, S. L., Mladenov, N., Symons, C. C., & Shurin, J. B. (2023). Fire transforms effects of terrestrial subsidies on aquatic ecosystem structure and function. *Global Change Biology*, 30, e17058. <https://doi.org/10.1111/gcb.17058>





## **Supplemental Materials**

### **Fire transforms effects of terrestrial subsidies on aquatic ecosystem structure and function**

Christopher B. Wall, Cody J. Spiegel, Evelyn M. Diaz, Cindy H. Tran, Alexia Fabiani, Taryn Y. Broe, Elisabet Perez-Coronel, Sara L. Jackrel, Natalie Mladenov, Ceila C. Symons, Jonathan B. Shurin

Corresponding author: Christopher B. Wall  
Email: [cwall@ucsd.edu](mailto:cwall@ucsd.edu)

#### **This PDF file includes:**

Supporting text  
Figures S1 to S12  
Tables S1 to S13

## Supporting Text

### Supplemental Results

#### *Dissolved oxygen percent*

Dissolved oxygen (DO as % O<sub>2</sub>) measurements showed consistent patterns among replicate dawn measurements (separated by 24 h) in each time point (Figure S6), although % O<sub>2</sub> showed considerable change over time. At Day-10, dawn and dusk % O<sub>2</sub> was consistently < 50 % in tanks receiving more than 100 g of plant material, with treatments > 200 g plant material showing hypoxic conditions (< 10 % O<sub>2</sub>). Significant non-linear relationships between % O<sub>2</sub> and plant biomass were observed in all time points, with treatment-specific intercepts for a global smoother at Day-10 and significant non-linear relationships that varied by treatment for dawn-and-dusk measurements at Days-31 and 59 (Tables S5 and S6). Measurements on Days-31 and 59 also showed significantly higher % O<sub>2</sub> in mid-range burned tanks (100 - 200 g) compared to unburned, however, % O<sub>2</sub> was consistently lower in burned treatments at 400 g compared to unburned tanks (Figure S7). By Day-89, treatment effects were minimal although % O<sub>2</sub> remained higher in tanks receiving less plant materials (Figure S6).

#### *Isotope labeling*

Nitrogen isotope labeling (<sup>15</sup>N) substantially increased the δ<sup>15</sup>N isotope values of pooled burned-and-unburned sage leaf materials (mean ± SD; 296 ± 53 ‰) relative to willow (13 ± 0.3 ‰) ( $p < 0.001$ ) (Figure S9, Table S9A). Burning treatment did not affect leaf δ<sup>15</sup>N values for sage ( $p = 0.423$ ) or willow ( $p = 0.485$ ). C:N values were higher in burned relative to unburned sage ( $p = 0.001$ ), driven by higher C:N values (~ 70) in sage subjected

to longer fire treatment (i.e., very-burned sage), but equivalent between burned and unburned willow ( $p=0.061$ ) (Figure S9A and Table S9A).  $\delta^{15}\text{N}$  values did not differ between burned and unburned sage ( $p=0.423$ ) or willow ( $p=0.485$ ). Using pooled burned and unburned leaves, sage had C:N values slightly higher than willow (mean 49 and 47) ( $p=0.014$ ) (Figure S9B). Plankton  $\delta^{15}\text{N}$  values were slightly lower than those in the plankton (11 vs. 13 ‰) ( $p=0.001$ ), and plankton C:N was significantly lower than willow (mean 5.8) ( $p<0.001$ ) (Figure S9B and Table S9A).

Plankton  $\delta^{15}\text{N}$  was used in isotope mixing models to determine the percent of sage- $^{15}\text{N}$  incorporated into plankton biomass. Raw  $\delta^{15}\text{N}$  values are reported in Figure S9C, D relative to the total dry plant material added to tanks.

**Supplemental Figures and Table**

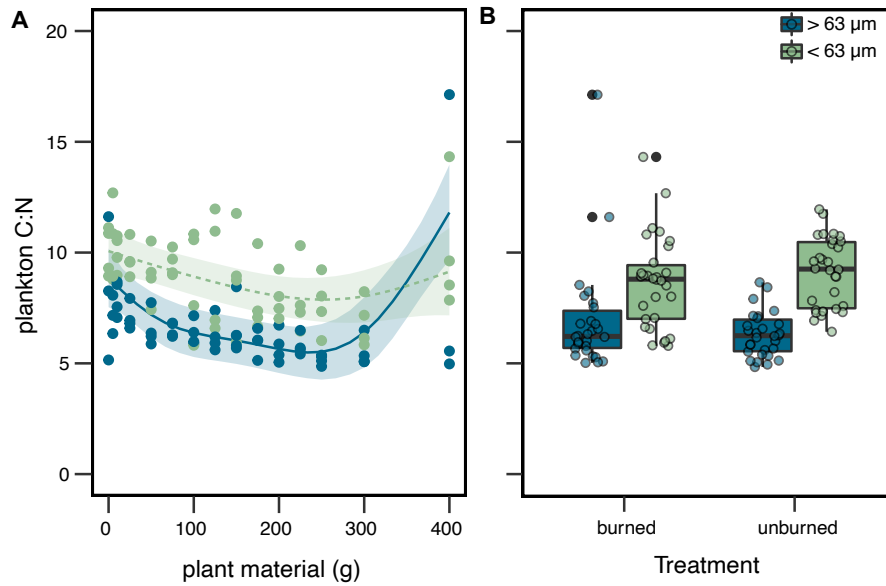


**Figure S1.** (A) Plankton C:N along the plant material gradient pooled across days (10 and 31) and treatments (burned and unburned), and (B) plankton C:N in treatment tanks receiving burned and unburned plant material. Lines best-fit generalized additive models (GAMs) (*left*) with treatment-level 95% confidence intervals. Box plots depict the median (bold center line), first and third quartiles (lower and upper bounds), whiskers (1.5x the distance between first and third quartiles), and outliers (black circles).

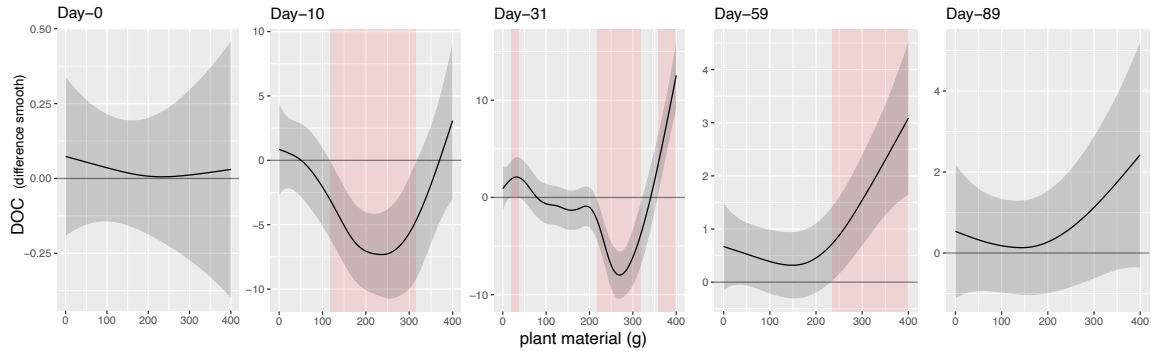


**Figure S2.** Model effects from GAMs with differences between smoothers for DOC concentration across time in treatments receiving burned and unburned plant material. Shaded regions are the confidence interval for ‘the difference smooth,’ which is the difference between burned and unburned treatment smoothers. Significant differences between treatment-level smoothers are noted in regions that do not include zero  $\pm$  model confidence intervals and are shaded in pink.

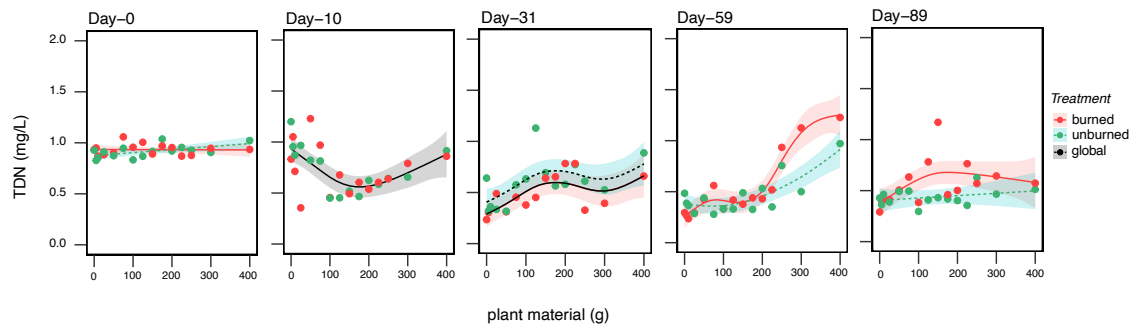


**Figure S3.** Total dissolved nitrogen (TDN) concentration across time in treatments receiving burned and unburned plant material. Lines represent best-fit GAMs with 95% confidence intervals. Black lines with gray confidence intervals indicate global smoothers across all data points; solid (*burned*) and dotted (*unburned*) black lines together represent treatment-level intercepts with global smoothers; colored lines indicate factor-smooths that vary between treatments.

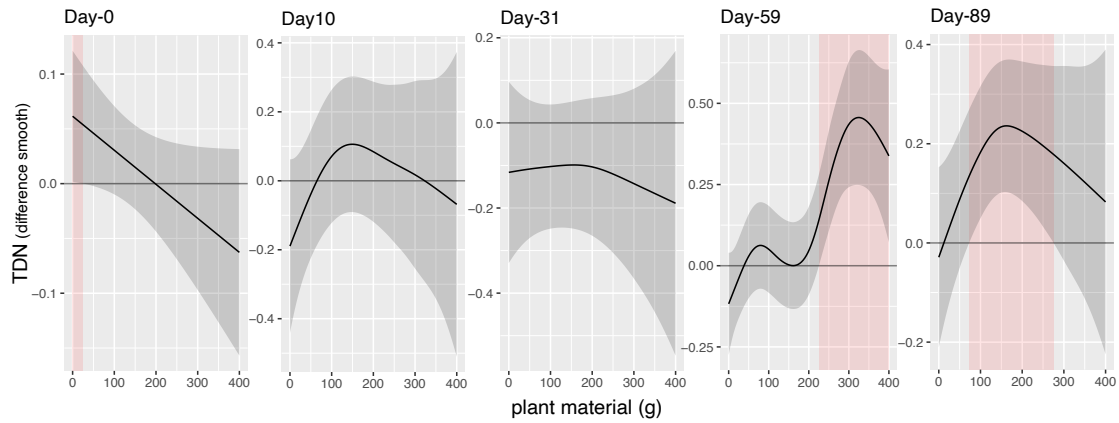


**Figure S4.** Model effects from GAMs with differences between smoothers for TN across time in treatments receiving burned and unburned plant material. Shaded regions are the confidence interval for ‘the difference smooth,’ which is the difference between burned and unburned treatment smoothers. Significant differences between treatment-level smoothers are noted in regions that do not include zero  $\pm$  model confidence intervals and are shaded in pink.

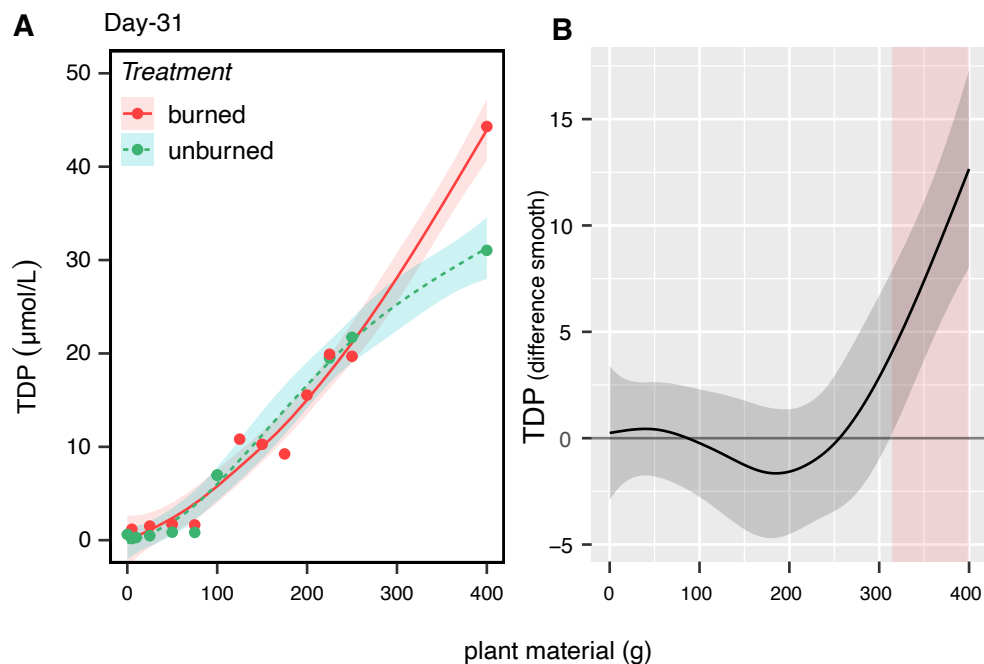


**Figure S5.** (A) Total phosphorus concentration in water from burned and unburned treatments at Day-31, and (B) the difference between burned and unburned treatment smoothers. Lines represent best-fit GAMs (*left*) with treatment-level 95% confidence intervals. Lines in B represent differences between treatment-level smoothers, where significant differences (shaded in pink) are noted in regions that do not include zero  $\pm$  model confidence intervals.



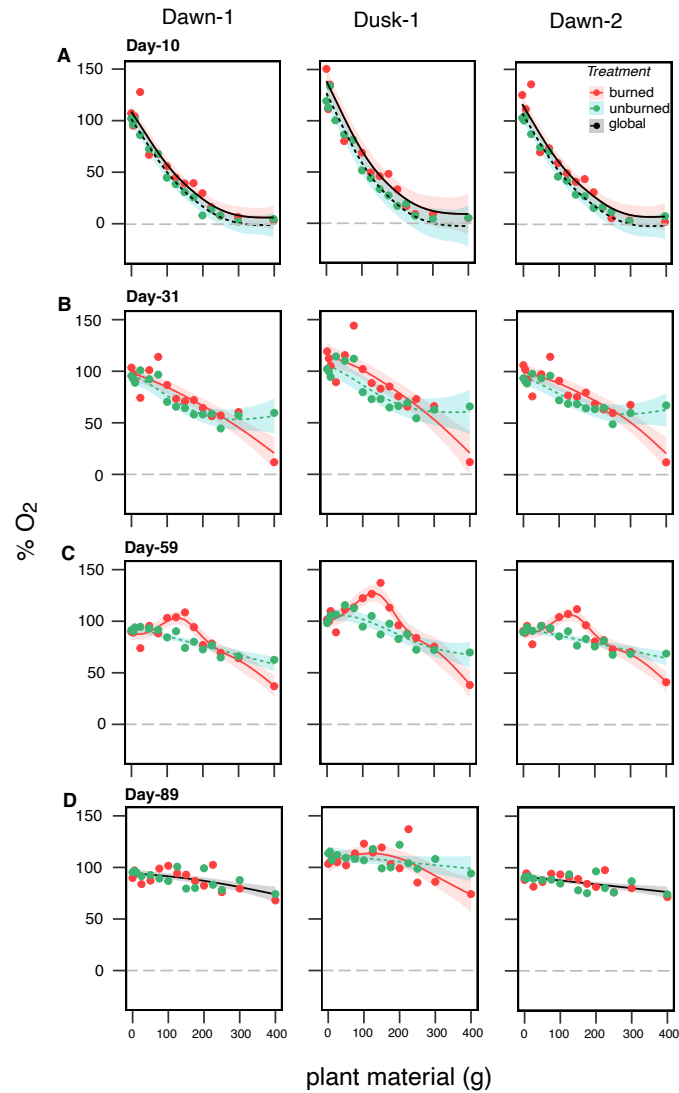


**Figure S6. (A-D)** Changes in dissolved oxygen concentration (%) at dawn and dusk across the four experimental periods. Data here were used to calculate net ecosystem production and respiration. Lines represent best-fit GAMs with treatment-level 95% confidence intervals. Black lines with gray confidence intervals indicate global smoothers across all data points; solid (*burned*) and dotted (*unburned*) black lines together represent treatment-level intercepts with global smoothers; colored lines indicate factor-smooths that vary between treatments.

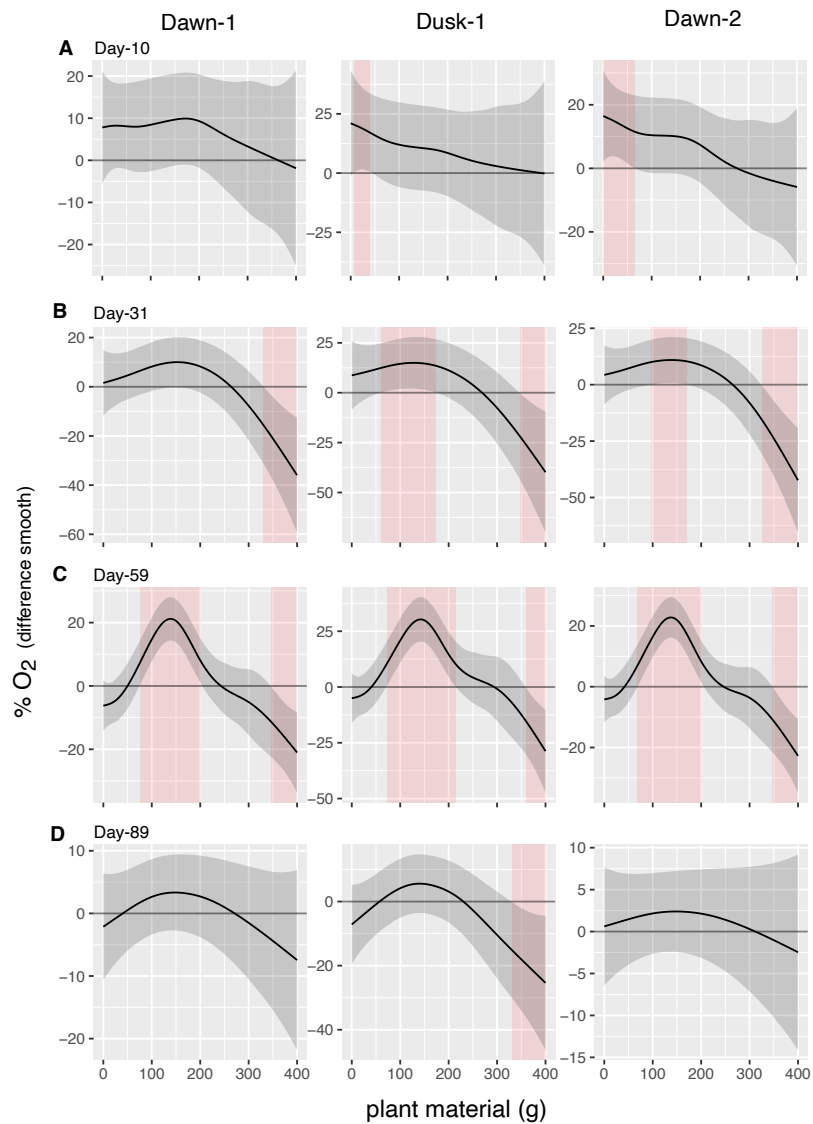


**Figure S7.** (A-D) Model effects from GAMs with differences between smoothers for oxygen concentration (% O<sub>2</sub>) across four experimental time points in treatments receiving burned and unburned plant material. Shaded regions are the confidence interval for ‘the difference smooth,’ which is the difference between burned and unburned treatment smoothers. Significant differences between treatment-level smoothers are noted in regions that do not include zero ± model confidence intervals and are shaded in pink.

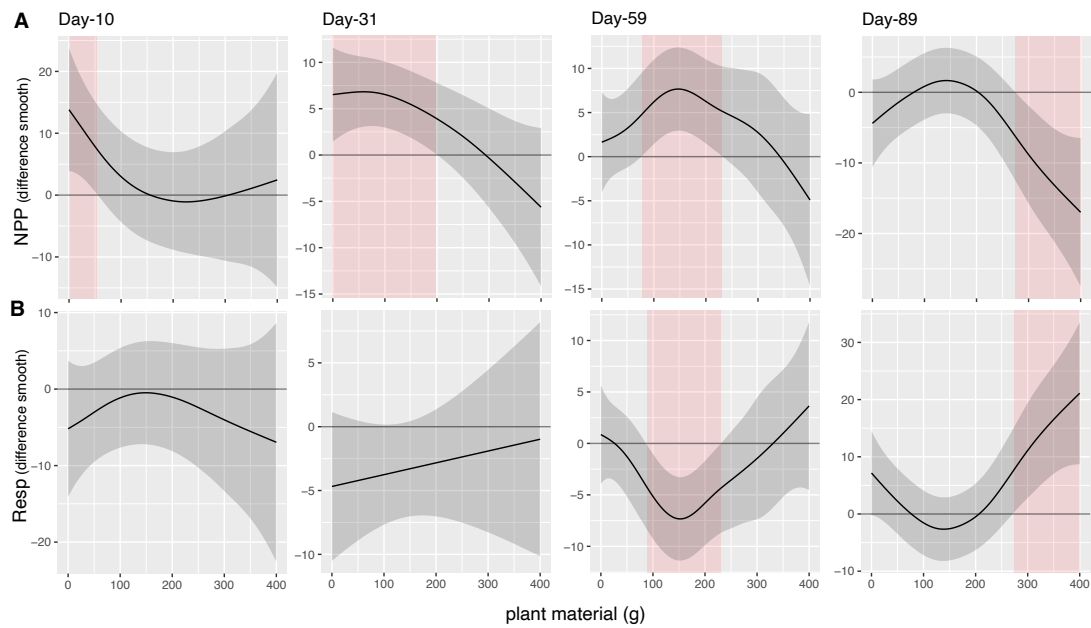


**Figure S8.** Model effects from GAMs with differences between smoothers for **(A)** net primary production (NPP) and **(B)** respiration (Resp) across time in treatments receiving burned and unburned plant material. Shaded regions are the confidence interval for ‘the difference smooth,’ which is the difference between burned and unburned treatment smoothers. Significant differences between treatment-level smoothers are noted in regions that do not include zero  $\pm$  model confidence intervals and are shaded in pink.

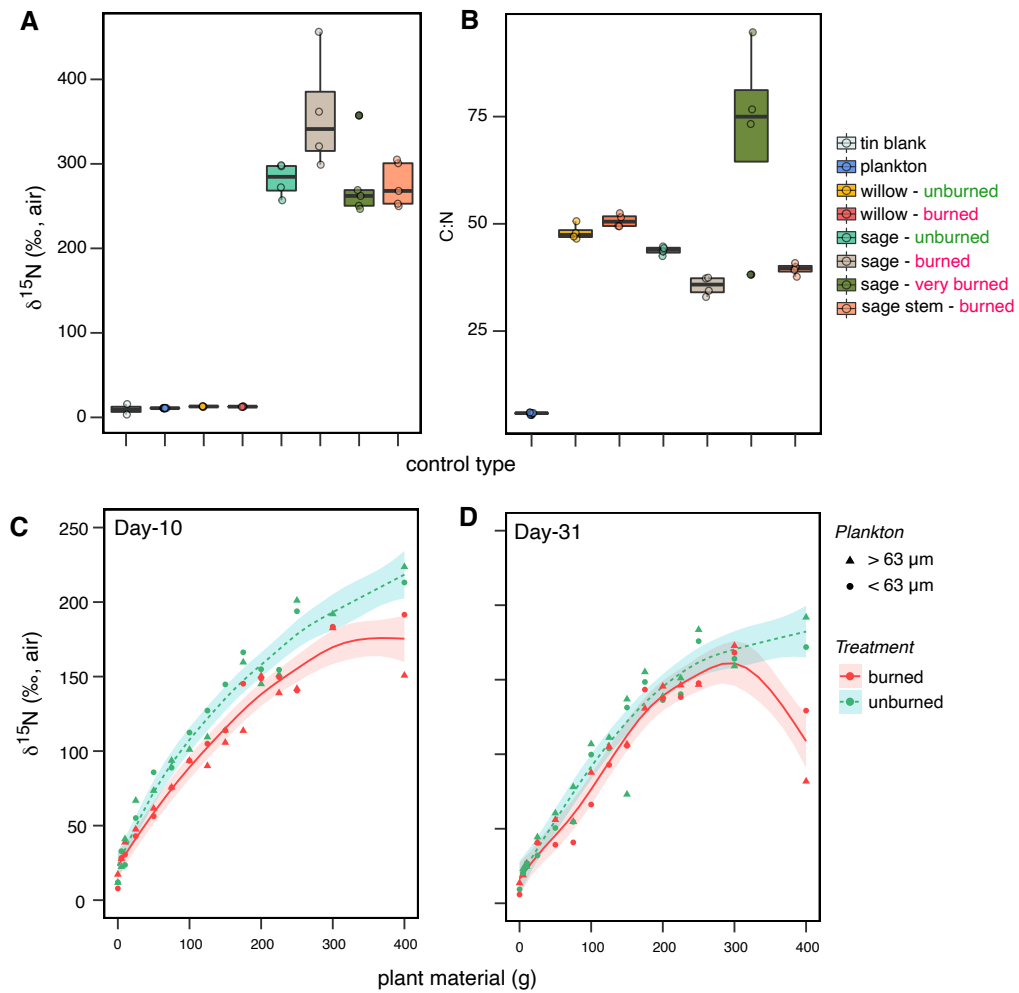


**Figure S9.** (A) Nitrogen isotope values and (B) C:N ratio for experimental controls (tin blanks), stock plankton, and burned or unburned plant material (willow, sage). (C, D) Nitrogen isotope values of plankton fractions in burned and unburned treatments at Day-10 (Time-1) and Day-31 (Time-2). Lines in the bottom panel represent best-fit GAMs with treatment-level 95% confidence intervals. Box plots depict the median (bold center line), first and third quartiles (lower and upper bounds), whiskers (1.5x the distance between first and third quartiles), and outliers (black circles).

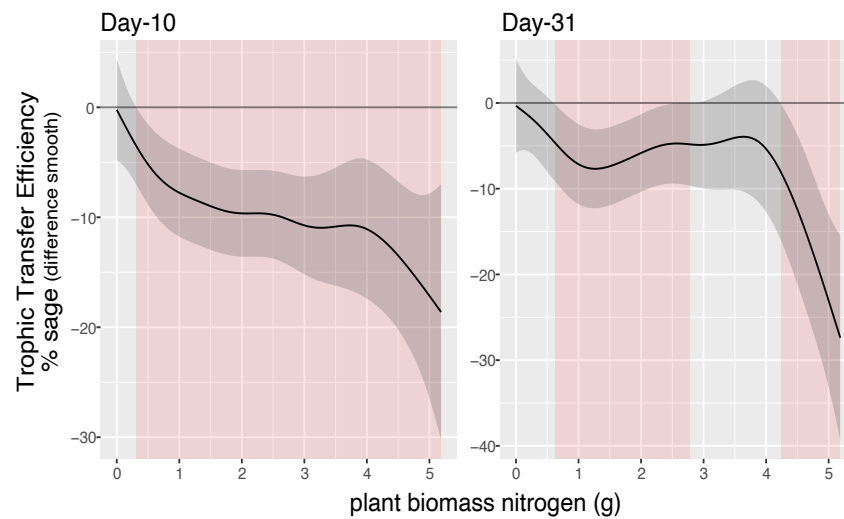


**Figure S10.** Model effects from GAMs with differences between smoothers for % sage-derived  $^{15}\text{N}$  at Day-10 and Day-31 in tanks receiving burned and unburned plant material. Significant differences between treatment-level smoothers are noted in regions that do not include zero  $\pm$  model confidence intervals and are shaded in pink.

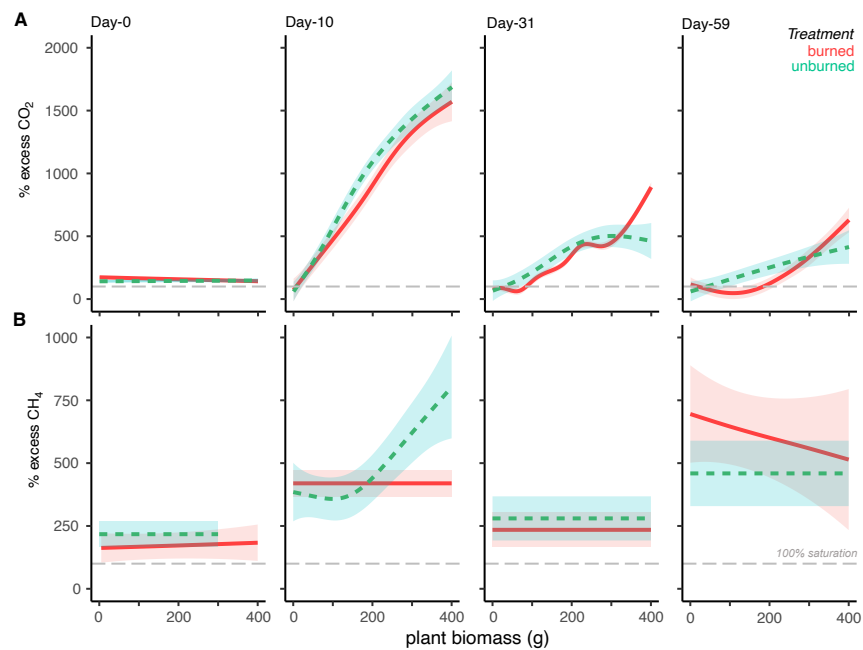


**Figure S11.** Percent excess concentrations for greenhouse gasses **(A)** carbon dioxide ( $\text{CO}_2$ ) and **(B)** methane ( $\text{CH}_4$ ) in tanks receiving burned and unburned plant material at the beginning of the experiment and during three experimental time points. Gray line indicates 100% saturation under atmospheric equilibrium.

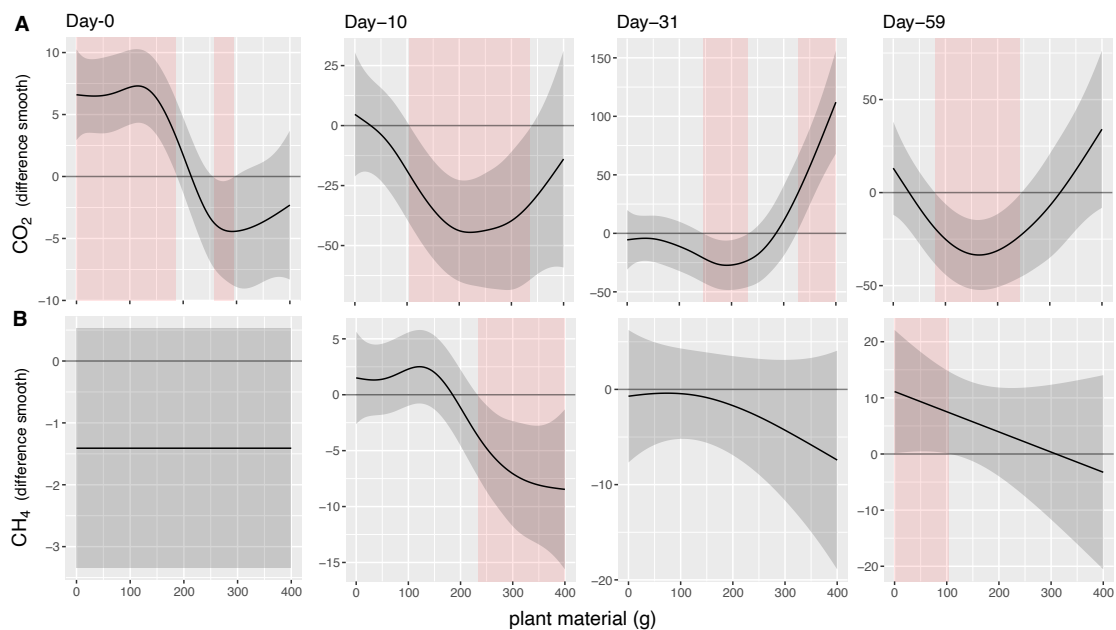


**Figure S12.** Model effects from GAMs with differences between smoothers for greenhouse gasses **(A)** carbon dioxide (CO<sub>2</sub>) and **(B)** methane (CH<sub>4</sub>) in tanks receiving burned and unburned plant material at the beginning of the experiment and during three experimental time points. Significant differences between treatment-level smoothers are noted in regions that do not include zero  $\pm$  model confidence intervals and are shaded in pink.

**Table S1.** Linear models testing the influence of treatment (burned vs. unburned) plant material (leaf, stem) on sage biomass prior to addition to aquatic mesocosms. Factor interactions were excluded, except for their three-way interaction, which allowed for *a priori* contrasts of burning effects within plant tissue types in a single species.

<i>Sage biomass</i>	<i>Effect</i>	<i>SS</i>	<i>df</i>	<i>F</i>	<i>p-value</i>
Nitrogen (%N)	Treatment	0.028	1	8.663	<b>0.019</b>
	Type	0.260	1	80.525	<b>&lt;0.001</b>
	Treatment:Type	0.071	1	21.810	<b>0.002</b>
	Residual	0.026	8		
Phosphorus (%P)	Treatment	0.001	1	1.968	0.198
	Type	0.008	1	19.306	<b>0.002</b>
	Treatment:Type	0.0001	1	0.144	0.714
	Residual	0.003	8		
Potassium (%K)	Treatment	0.256	1	7.616	<b>0.025</b>
	Type	0.180	1	5.357	<b>0.049</b>
	Treatment:Type	0.074	1	2.188	0.177
	Residual	0.269	8		
Sulfur (%S)	Treatment	0.0001	1	0.132	0.726
	Type	0.112	1	141.389	<b>&lt;0.001</b>
	Treatment:Type	0.0004	1	0.489	0.504
	Residual	0.006	8		
Zinc (Zn ppm)	Treatment	3,073	1	2.336	0.165
	Type	3,281	1	2.494	0.153
	Treatment:Type	1,236	1	0.940	0.361
	Residual	10,524	8		

ANOVA table generated from Type-III sum of squares using *car* package in R. *SS* = sum of squares; *df* = degrees of freedom; *MS* = mean sum of squares. Significant effects ( $p < 0.05$ ) are in bold.



**Table S2.** Linear models testing the influence of treatment (burned vs. unburned) plant material (leaf, stem) on willow biomass prior to addition to aquatic mesocosms. Factor interactions were excluded, except for their three-way interaction, which allowed for *a priori* contrasts of burning effects within plant tissue types in a single species.

<i>Willow biomass</i>	<i>Effect</i>	<i>SS</i>	<i>df</i>	<i>F</i>	<i>p-value</i>
Nitrogen (%N)	Treatment	0.082	1	6.019	<b>0.044</b>
	Type	1.454	1	107.153	<b>&lt;0.001</b>
	Treatment:Type	0.044	1	3.212	0.116
	Residual	0.095	7		
Phosphorus (%P)	Treatment	0.006	1	18.283	<b>0.004</b>
	Type	0.007	1	20.670	<b>0.003</b>
	Treatment:Type	0.001	1	2.513	0.157
	Residual	0.002	7		
Potassium (%K)	Treatment	0.068	1	8.034	<b>0.025</b>
	Type	0.264	1	31.358	<b>&lt;0.001</b>
	Treatment:Type	0.002	1	0.173	0.690
	Residual	0.059	7		
Sulfur (%S)	Treatment	0.003	1	22.303	<b>0.002</b>
	Type	0.042	1	374.819	<b>&lt;0.001</b>
	Treatment:Type	0.001	1	11.985	<b>0.011</b>
	Residual	0.001	7		
Zinc (Zn ppm)	Treatment	22,363	1	35.304	<b>&lt;0.001</b>
	Type	21,956	1	34.663	<b>&lt;0.001</b>
	Treatment:Type	5,340	1	8.431	<b>0.023</b>
	Residual	4,434	7		

ANOVA table generated from Type-III sum of squares using *car* package in R. *SS* = sum of squares; *df* = degrees of freedom; *MS* = mean sum of squares. Significant effects ( $p < 0.05$ ) are in bold.

**Table S3.** Model selection for percent dissolved organic carbon (DOC), total dissolved nitrogen (TDN), and total dissolved phosphorus (TDP) with candidate GAM models\* assessed in each time point, corresponding to 0, 10, 31, 59, and 89 days post addition of burned or unburned plant material to experimental mesocosms. TDP was only measured at Day-31.

<i>Metric</i>	<i>Time</i>	<i>Model</i>	<i>df</i>	<i>AIC</i>	<i>ΔAIC</i>
<b>DOC</b>	Day-0	~Treatment + s(plant material, by= Treatment)	5.5	3.2	
		~Treatment + s(plant material)	4.0	1.0	
		~s(plant material)	3.1	<b>-0.8</b>	0.0
	Day-10	~Treatment + s(plant material, by= Treatment)	10.9	<b>146.8</b>	-15.2
		~Treatment + s(plant material)	6.6	157.8	
		~s(plant material)	5.5	162.0	
	Day-31	~Treatment + s(plant material, by= Treatment)	12.5	<b>117.7</b>	-40.3
		~Treatment + s(plant material)	6.3	160.0	
		~s(plant material)	5.3	158.0	
	Day-59	~Treatment + s(plant material, by= Treatment)	8.2	<b>64.0</b>	-12.1
		~Treatment + s(plant material)	4.0	69.7	
		~s(plant material)	3.0	76.1	
	Day-89	~Treatment + s(plant material, by= Treatment)	6.3	110.9	
		~Treatment + s(plant material)	5.4	109.3	
		~s(plant material)	4.4	<b>108.6</b>	0.0
<b>TDN</b>	Day-0	~Treatment + s(plant material, by= Treatment)	5.0	<b>-85.1</b>	-0.6
		~Treatment + s(plant material)	4.0	-83.4	
		~s(plant material)	3.0	-84.5	
	Day-10	~Treatment + s(plant material, by= Treatment)	8.9	-7.8	
		~Treatment + s(plant material)	6.2	-10.6	
		~s(plant material)	5.3	<b>-12.6</b>	0.0
	Day-31	~Treatment + s(plant material, by= Treatment)	6.3	-11.7	
		~Treatment + s(plant material)	6.9	<b>-18.1</b>	-3.0
		~s(plant material)	5.5	-15.0	
	Day-59	~Treatment + s(plant material, by= Treatment)	11.3	<b>-39.6</b>	-13.6
		~Treatment + s(plant material)	6.1	-26.2	
		~s(plant material)	5.1	-26.0	
	Day-89	~Treatment + s(plant material, by= Treatment)	7.0	<b>-23.7</b>	-6.4
		~Treatment + s(plant material)	4.8	-20.6	
		~s(plant material)	3.6	-17.4	
<b>TDP</b>	Day-31	Treatment + s(plant material, by=Treatment)	9.9	<b>100.1</b>	-16.8
		Treatment + s(plant material)	5.9	117.9	
		s(plant material)	4.8	116.9	

\**Treatment + s(plant material, by= Treatment)* GAM has parametric terms (*Treatment*) and separate smoothers for each treatment. *Treatment + s(plant material)* GAM has a global smoother allowing for off-set intercepts according to treatments. The *s(plant material)* GAM fits a global smoother to all data. **Bold** represents the selected models. Delta AIC ( $\Delta AIC$ ) is the difference between the selected model and the global smoother model.

**Table S4.** Generalized additive models (GAM) testing treatment (burned vs. unburned) and factor-smooth interaction effects on dissolved organic carbon (DOC) and total dissolved nitrogen (TDN) at five time points and total phosphorus (TP) at one time point. Separate smoothers were fit for burned and unburned data, and ANOVA tables were generated by *anova.gam()*.

<b>Dissolved organic carbon (DOC mg/L)</b>					
	<i>Effect</i>	<i>df/edf</i>	<i>Ref.df</i>	<i>F</i>	<i>p-value</i>
Day-0	s(plant material)	1.040	1.080	1.341	0.240
Day-10	Treatment	1	–	9.571	<b>0.005</b>
	s(plant material) : burned	3.623	4.412	119.7	<b>&lt;0.001</b>
	s(plant material) : unburned	3.151	3.853	149.1	<b>&lt;0.001</b>
Day-31	Treatment	1	–	0.035	0.853
	s(plant material) : burned	6.482	7.532	34.39	<b>&lt;0.001</b>
	s(plant material) : unburned	1.568	1.929	59.34	<b>&lt;0.001</b>
Day-59	Treatment	1	–	12.32	<b>0.002</b>
	s(plant material) : burned	2.051	2.532	94.00	<b>&lt;0.001</b>
	s(plant material) : unburned	2.202	2.714	56.55	<b>&lt;0.001</b>
Day-89	s(plant material)	1.928	2.385	29.80	<b>&lt;0.001</b>
<b>Total dissolved nitrogen (TDN mg/L)</b>					
Day-0	Treatment	1	–	0.879	0.357
	s(plant material) : burned	1.000	1.000	0.009	0.927
	s(plant material) : unburned	1.000	1.000	6.303	<b>0.019</b>
Day-10	s(plant material)	2.848	3.492	5.720	<b>0.003</b>
Day-31	Treatment	1	–	4.122	0.053
	s(plant material)	3.207	3.921	4.870	<b>0.004</b>
Day-59	Treatment	1	–	3.500	0.075
	s(plant material) : burned	4.359	5.269	23.03	<b>&lt;0.001</b>
	s(plant material) : unburned	2.457	3.022	10.52	<b>&lt;0.001</b>
Day-89	Treatment	1	–	6.231	<b>0.020</b>
	s(plant material) : burned	2.417	2.973	3.613	<b>0.032</b>
	s(plant material) : unburned	1.000	1.000	0.531	0.473
<b>Total dissolved phosphorus (TDP <math>\mu\text{mol/L}</math>)</b>					
Day-31	Treatment	1	–	1.329	0.267
	s(plant material) : burned	2.924	3.525	154.7	<b>&lt;0.001</b>
	s(plant material) : unburned	2.930	3.371	124.6	<b>&lt;0.001</b>

*Treatment* indicates the parametric term in GAM, *s(plant material)* is the smooth term for either burned or unburned treatments. *df/edf* column indicates either *df* (degrees of freedom) for parametric terms or *edf* (effective degrees of freedom) for smoother terms; *Ref.df* = reference degree of freedom, where dashes indicate NA for parametric terms. Significant effects ( $p < 0.05$ ) are in bold.

**Table S5.** Model selection for percent dissolved oxygen (DO as % O<sub>2</sub>) with candidate GAM models\* assessed in each time point, corresponding to Days-10, 31, 59, and 89 post addition of burned or unburned plant material to experimental mesocosms. Dawn and dusk measurements represent discrete back-to-back measurements over a 24 h period.

<i>Metric</i>	<i>Time</i>		<i>Model</i>	<i>df</i>	<i>AIC</i>	<i>ΔAIC</i>
% O <sub>2</sub>	Day-10	dawn-1	~Treatment + s(plant material, by= Treatment)	9.7	226.4	
			~Treatment + s(plant material)	6.7	<b>221.5</b>	-3.9
			~s(plant material)	5.6	225.4	
		dusk-1	~Treatment + s(plant material, by= Treatment)	9.3	258.5	
			~Treatment + s(plant material)	6.5	<b>254.3</b>	-3.1
			~s(plant material)	5.4	257.4	
		dawn-2	~Treatment + s(plant material, by= Treatment)	9.9	230.6	
			~Treatment + s(plant material)	6.8	<b>228.9</b>	-4.7
			~s(plant material)	5.6	233.6	
	Day-31	dawn-1	~Treatment + s(plant material, by= Treatment)	8.4	<b>231.2</b>	-4.8
			~Treatment + s(plant material)	4.0	237.8	
			~s(plant material)	3.0	236.0	
		dusk-1	~Treatment + s(plant material, by= Treatment)	8.2	<b>246.9</b>	-4.3
			~Treatment + s(plant material)	4.0	251.7	
			~s(plant material)	3.0	251.2	
		dawn-2	~Treatment + s(plant material, by= Treatment)	8.8	<b>229.5</b>	-7.4
			~Treatment + s(plant material)	4.0	238.5	
			~s(plant material)	3.0	237.0	
	Day-59	dawn-1	~Treatment + s(plant material, by= Treatment)	10.0	<b>198.3</b>	-22.8
			~Treatment + s(plant material)	6.5	222.3	
			~s(plant material)	5.5	221.1	
		dusk-1	~Treatment + s(plant material, by= Treatment)	12.4	<b>215.3</b>	-22.9
			~Treatment + s(plant material)	6.9	237.2	
			~s(plant material)	5.9	238.2	
dawn-2		~Treatment + s(plant material, by= Treatment)	10.2	<b>195.7</b>	-25.4	
		~Treatment + s(plant material)	6.6	221.4		
		~s(plant material)	5.5	221.1		
Day-89	dawn-1	~Treatment + s(plant material, by= Treatment)	6.5	208.2		
		~Treatment + s(plant material)	5.0	208.2		
		~s(plant material)	4.1	<b>206.3</b>	0.0	
	dusk-1	~Treatment + s(plant material, by= Treatment)	7.1	<b>229.0</b>	-2.0	
		~Treatment + s(plant material)	5.6	232.5		
		~s(plant material)	4.7	231.0		
	dawn-2	~Treatment + s(plant material, by= Treatment)	6.0	198.5		
		~Treatment + s(plant material)	4.0	196.6		
		~s(plant material)	3.1	<b>195.0</b>	0.0	

\**Treatment + s(plant material, by= Treatment)* GAM has parametric terms (*Treatment*) and separate smoothers for each treatment. *Treatment + s(plant material)* GAM has a global smoother allowing for off-set intercepts according to treatments. The *s(plant material)* GAM fits a global smoother to all data. **Bold** represents the selected models. Delta AIC (*ΔAIC*) is the difference between the selected model and the global smoother model.

**Table S6.** Generalized additive models (GAM) testing treatment (burned vs. unburned) and factor-smooth interaction effects on dissolved oxygen measured at dawn, dusk, and dawn over a 24 h period. Separate smoothers were fit for burned and unburned data, and ANOVA tables were generated by *anova.gam()*.

<b>Dissolved oxygen (% O<sub>2</sub>)</b>						
		<i>Effect</i>	<i>df/edf</i>	<i>Ref.df</i>	<i>F</i>	<i>p-value</i>
Day-10	dawn-1	Treatment	1	–	5.467	<b>0.028</b>
		<i>s(plant material)</i>	3.516	4.287	127.7	<b>&lt;0.001</b>
	dusk-1	Treatment	1	–	4.718	<b>0.040</b>
		<i>s(plant material)</i>	3.225	3.942	73.89	<b>&lt;0.001</b>
	dawn-2	Treatment	1	–	6.333	<b>0.019</b>
		<i>s(plant material)</i>	3.481	4.245	114.0	<b>&lt;0.001</b>
Day-31	dawn-1	Treatment	1	–	0.309	0.584
		<i>s(plant material) : burned</i>	1.844	2.282	32.91	<b>&lt;0.001</b>
		<i>s(plant material) : unburned</i>	2.508	3.083	14.25	<b>&lt;0.001</b>
	dusk-1	Treatment	1	–	1.887	0.182
		<i>s(plant material) : burned</i>	2.026	2.503	25.65	<b>&lt;0.001</b>
		<i>s(plant material) : unburned</i>	2.190	2.699	10.07	<b>&lt;0.001</b>
	dawn-2	Treatment	1	–	0.744	0.397
		<i>s(plant material) : burned</i>	2.289	2.818	27.35	<b>&lt;0.001</b>
		<i>s(plant material) : unburned</i>	2.411	2.966	10.64	<b>&lt;0.001</b>
Day-59	dawn-1	Treatment	1	–	1.656	0.212
		<i>s(plant material) : burned</i>	4.970	5.958	23.28	<b>&lt;0.001</b>
		<i>s(plant material) : unburned</i>	1.000	1.000	52.88	<b>&lt;0.001</b>
	dusk-1	Treatment	1	–	6.275	<b>0.021</b>
		<i>s(plant material) : burned</i>	5.038	6033	24.8	<b>&lt;0.001</b>
		<i>s(plant material) : unburned</i>	2.753	3.377	14.67	<b>&lt;0.001</b>
	dawn-2	Treatment	1	–	3.860	<b>0.062</b>
		<i>s(plant material) : burned</i>	5.166	6.175	22.80	<b>&lt;0.001</b>
		<i>s(plant material) : unburned</i>	1.000	1.000	38.78	<b>&lt;0.001</b>
Day-89	dawn-1	<i>s(plant material)</i>	1.667	2.061	9.333	<b>&lt;0.001</b>
	dusk-1	Treatment	1	–	0.506	0.483
		<i>s(plant material) : burned</i>	2.575	3.163	5.636	<b>0.004</b>
		<i>s(plant material) : unburned</i>	1.000	1.000	2.538	0.124
	dawn-2	<i>s(plant material)</i>	1.041	1.081	15.09	<b>&lt;0.001</b>

*Treatment* indicates the parametric term in GAM, *s(plant material)* is the smooth term for either burned or unburned treatments. *df*= degrees of freedom for parametric terms; *edf*= effective degrees of freedom for smoother terms; *Ref.df*= reference degree of freedom, where dashes indicate NA for parametric terms. Significant effects ( $p < 0.05$ ) are in bold.

**Table S7.** Model selection for net primary productivity (NPP) and respiration (Resp) with candidate GAM models\* assessed at four time points post addition of burned or unburned plant material to experimental mesocosms.

<i>Metric</i>	<i>Time</i>	<i>Model</i>	<i>df</i>	<i>AIC</i>	<i>ΔAIC</i>
NPP	Day-10	~Treatment + s(plant material, by= Treatment)	8.1	214.2	-0.9
		~Treatment + s(plant material)	6.1	<b>213.5</b>	
		~s(plant material)	5.0	214.4	
	Day-31	~Treatment + s(plant material, by= Treatment)	6.4	177.5	-9.3
		~Treatment + s(plant material)	7.7	<b>176.3</b>	
		~s(plant material)	4.2	185.6	
	Day-59	~Treatment + s(plant material, by= Treatment)	11.0	175.7	-6.0
		~Treatment + s(plant material)	7.3	<b>175.2</b>	
		~s(plant material)	6.1	181.2	
	Day-89	~Treatment + s(plant material, by= Treatment)	7.4	<b>187.4</b>	-5.2
		~Treatment + s(plant material)	5.8	192.2	
		~s(plant material)	4.8	192.5	
Resp	Day-10	~Treatment + s(plant material, by= Treatment)	8.0	207.9	0.0
		~Treatment + s(plant material)	6.1	203.6	
		~s(plant material)	5.1	<b>203.3</b>	
	Day-31	~Treatment + s(plant material, by= Treatment)	5.0	189.6	-6.4
		~Treatment + s(plant material)	9.6	<b>173.3</b>	
		~s(plant material)	8.3	179.7	
	Day-59	~Treatment + s(plant material, by= Treatment)	11.6	<b>164.9</b>	-5.8
		~Treatment + s(plant material)	7.4	167.6	
		~s(plant material)	6.3	170.8	
	Day-89	~Treatment + s(plant material, by= Treatment)	7.5	<b>196.9</b>	-7.0
		~Treatment + s(plant material)	6.0	202.9	
		~s(plant material)	4.9	203.9	

\**Treatment + s(plant material, by= Treatment)* GAM has parametric terms (*Treatment*) and separate smoothers for each treatment. *Treatment + s(plant material)* GAM has a global smoother allowing for off-set intercepts according to treatments. The *s(plant material)* GAM fits a global smoother to all data. **Bold** represents the selected models. Delta AIC ( $\Delta AIC$ ) is the difference between the selected model and the global smoother model.

**Table S8.** Generalized additive models (GAM) testing treatment (burned vs. unburned) and factor-smooth interaction effects on net primary productivity (NPP) and respiration (Resp) at four time points following the addition of plant material to experimental mesocosm. Separate smoothers were fit for burned and unburned data, and ANOVA tables were generated by *anova.gam()*.

<b>Net primary productivity (NPP <math>\Delta</math> % O<sub>2</sub>)</b>					
	<i>Effect</i>	<i>df/edf</i>	<i>Ref.df</i>	<i>F</i>	<i>p-value</i>
Day-10	Treatment	1	–	2.626	0.117
	<i>s</i> (plant material)	2.552	3.136	15.760	<b>&lt;0.001</b>
Day-31	Treatment	1	–	8.479	<b>0.007</b>
	<i>s</i> (plant material)	3.867	4.699	4.856	<b>0.006</b>
Day-59	Treatment	1	–	7.304	<b>0.012</b>
	<i>s</i> (plant material)	3.719	4.525	8.277	<b>&lt;0.001</b>
Day-89	Treatment	1	–	2.620	0.118
	<i>s</i> (plant material) : burned	2.757	3.382	3.717	<b>0.020</b>
	<i>s</i> (plant material) : unburned	1.000	1.000	1.002	0.327
<b>Respiration (Resp <math>\Delta</math> % O<sub>2</sub>)</b>					
Day-10	Treatment	1	–	1.520	0.229
	<i>s</i> (plant material)	2.533	3.113	13.000	<b>&lt;0.001</b>
Day-31	Treatment	1	–	6.443	<b>0.019</b>
	<i>s</i> (plant material)	5.710	6.758	10.000	<b>&lt;0.001</b>
Day-59	Treatment	1	–	5.669	<b>0.027</b>
	<i>s</i> (plant material) : burned	3.762	4.576	13.144	<b>&lt;0.001</b>
	<i>s</i> (plant material) : unburned	3.274	4.000	7.775	<b>&lt;0.001</b>
Day-89	Treatment	1	–	3.380	0.078
	<i>s</i> (plant material) : burned	2.927	3.587	5.293	<b>0.004</b>
	<i>s</i> (plant material) : unburned	1.000	1.000	0.002	0.965

*Treatment* indicates the parametric term in GAM, *s*(plant material) is the smooth term for either burned or unburned treatments. *df*= degrees of freedom for parametric terms; *edf*= effective degrees of freedom for smoother terms; *Ref.df*= reference degree of freedom, where dashes indicate NA for parametric terms. Significant effects ( $p < 0.05$ ) are in bold.

**Table S9.** Non-parametric Mann-Whitney *U*-test and linear models testing effects of treatments (burned vs. unburned) and sample types ( $^{15}\text{N}$ -labeled sage, non-labeled willow, and plankton stock) on nitrogen isotope values ( $\delta^{15}\text{N}$ ) and C:N ratios prior to the start of the experiment (Day-0).

<b>Mann-Whitney <i>U</i>-tests</b>							
<i>Metric</i>	<i>Material</i>	<i>Contrast</i>		<i>U</i>	<i>p-value</i>		
$\delta^{15}\text{N}$	Leaf material	willow vs. sage		315	< <b>0.001</b>		
C:N				160	<b>0.014</b>		
$\delta^{15}\text{N}$	Willow, plankton	willow vs. plankton stock		28	<b>0.001</b>		
C:N				28	<b>0.001</b>		
<b>Linear models</b>							
<i>Metric</i>	<i>Material</i>	<i>Effect</i>	<i>df</i>	<i>SS</i>	<i>MS</i>	<i>F</i>	<i>p-value</i>
sage- $\delta^{15}\text{N}$	Leaf material	Treatment	2	5,178	2,589	0.913	0.423
		Residual	15	42,461	2,837		
sage-C:N		Treatment	2	3,011	1,505	11.320	<b>0.001</b>
		Residual	13	1729	133		
willow- $\delta^{15}\text{N}$		Treatment	1	0.050	0.050	0.554	0.485
		Residual	6	0.538	0.090		
willow-C:N		Treatment	1	14.773	14.773	5.279	0.061
		Residual	6	16.789	2.798		

Sample size is  $n=7$  (plankton),  $n=18$  (sage),  $n=8$  (willow).



**Table S10.** Model selection using plankton of two size classes (< 63 and > 63  $\mu\text{m}$ ) and measuring the trophic transfer (percent sage- $^{15}\text{N}$ ) in plankton biomass determined using a two-member mixing model and their stable isotope values ( $\delta^{15}\text{N}$ ). Candidate GAM models\* were assessed in two each time points post addition of burned or unburned plant material to experimental mesocosms.

<i>Metric</i>	<i>Time</i>	<i>Model</i>	<i>df</i>	<i>AIC</i>	<i><math>\Delta\text{AIC}</math></i>
% sage- $^{15}\text{N}$	Day-10	Treatment + Type + s(plant material, by=Treatment)	12.9	<b>354.1</b>	-26.7
		Treatment + Type + s(plant material)	8.7	359.8	
		s(plant material)	6.0	380.8	
	Day-31	Treatment + Type + s(plant material, by=Treatment)	12.8	<b>367.5</b>	-24.1
		Treatment + Type + s(plant material)	8.2	385.6	
		s(plant material)	6.1	391.6	
$\delta^{15}\text{N}$	Day-10	Treatment + Type + s(plant material, by=Treatment)	12.9	<b>479.4</b>	-26.7
		Treatment + Type + s(plant material)	8.7	485.1	
		s(plant material)	6.0	506.1	
	Day-31	Treatment + Type + s(plant material, by=Treatment)	12.8	<b>492.7</b>	-24.1
		Treatment + Type + s(plant material)	8.2	510.8	
		s(plant material)	6.1	516.8	

\* *Treatment + Type* represent parametric terms that provide offsets for either separate smoothers for each treatment *s(plant material, by=Treatment)* or global smoothers *s(plant material)*. **Bold** represents the selected models. Delta AIC ( $\Delta\text{AIC}$ ) is the difference between the selected model and the global smoother model.

**Table S11.** Generalized additive models (GAM) testing treatment (burned vs. unburned) and type (< 63  $\mu\text{m}$ , > 63  $\mu\text{m}$ ) and factor-smooth interaction effects on trophic transfer (plankton percent sage- $^{15}\text{N}$ ) calculated from a two-member mixing model. Separate smoothers were fit for burned and unburned data, and ANOVA tables were generated by *anova.gam()*.

<b>Plankton % sage-<math>^{15}\text{N}</math></b>					
	<i>Effect</i>	<i>df / edf</i>	<i>Ref.df</i>	<i>F</i>	<i>p-value</i>
Day-10	Treatment	1	–	31.261	<b>&lt;0.001</b>
	Type	1	–	1.721	0.196
	s(plant material) : burned	3.560	4.338	136.8	<b>&lt;0.001</b>
	s(plant material) : unburned	3.921	4.762	173.6	<b>&lt;0.001</b>
Day-31	Treatment	1	–	13.082	<b>&lt;0.001</b>
	Type	1	–	1.004	0.321
	s(plant material) : burned	4.669	5.621	79.45	<b>&lt;0.001</b>
	s(plant material) : unburned	3.34	4.082	125.45	<b>&lt;0.001</b>

*Treatment* indicates the parametric term in GAM, *s(plant material)* is the smooth term for either burned or unburned treatments. *df / edf* column indicates either *df* (degrees of freedom) for parametric terms or *edf* (effective degrees of freedom) for smoother terms; *Ref.df*= reference degree of freedom, where dashes indicate NA for parametric terms. Significant effects ( $p < 0.05$ ) are in bold.

**Table S12.** Model selection for greenhouse gas concentrations – carbon dioxide (CO<sub>2</sub> μM) and methane (CH<sub>4</sub> nM) – with candidate GAM models\* assessed before and after (three time points) the addition of burned or unburned plant material to experimental mesocosms.

<i>Metric</i>	<i>Time</i>	<i>Model</i>	<i>df</i>	<i>AIC</i>	<i>ΔAIC</i>
CO <sub>2</sub>	Day-0	Treatment +s(plant material, by=Treatment)	8.8	<b>153.1</b>	-20.4
		Treatment + s(plant material)	4.0	168.0	
		s(plant material)	3.0	173.4	
	Day-10	Treatment +s(plant material, by=Treatment)	9.2	<b>269.4</b>	-9.1
		Treatment + s(plant material)	6.6	272.2	
		s(plant material)	5.4	278.6	
	Day-31	Treatment +s(plant material, by=Treatment)	10.2	<b>266.6</b>	-15.8
		Treatment + s(plant material)	4.0	284.2	
		s(plant material)	3.0	282.4	
Day-59	Treatment +s(plant material, by=Treatment)	7.2	<b>270.2</b>	-10.0	
	Treatment + s(plant material)	5.4	280.3		
	s(plant material)	4.3	280.2		
CH <sub>4</sub>	Day-0	Treatment +s(plant material, by=Treatment)	5.0	132.9	-0.2
		Treatment + s(plant material)	4.0	<b>131.5</b>	
		s(plant material)	3.0	131.7	
	Day-10	Treatment +s(plant material, by=Treatment)	9.3	<b>159.6</b>	-5.3
		Treatment + s(plant material)	6.0	166.7	
		s(plant material)	5.1	164.9	
	Day-31	Treatment +s(plant material, by=Treatment)	5.9	198.2	0.0
		Treatment + s(plant material)	4.0	196.7	
		s(plant material)	3.0	<b>195.4</b>	
	Day-59	Treatment +s(plant material, by=Treatment)	5.0	227.7	-2.3
		Treatment + s(plant material)	7.1	<b>223.7</b>	
		s(plant material)	5.9	226.0	

\**Treatment + s(plant material, by= Treatment)* GAM has parametric terms (*Treatment*) and separate smoothers for each treatment. *Treatment + s(plant material)* GAM has a global smoother allowing for off-set intercepts according to treatments. The *s(plant material)* GAM fits a global smoother to all data. *Bold* represents the selected models. Delta AIC (*ΔAIC*) is the difference between the selected model and the global smoother model

**Table S13.** Generalized additive models (GAM) testing treatment (burned vs. unburned) and factor-smooth interaction effects on carbon dioxide (CO<sub>2</sub>) and methane (CH<sub>4</sub>) emissions from experimental mesocosms. Separate smoothers were fit for burned and unburned data, and ANOVA tables were generated by *anova.gam()*.

<b>Carbon dioxide (µM)</b>					
	<i>Effect</i>	<i>df/edf</i>	<i>Ref.df</i>	<i>F</i>	<i>p-value</i>
Day-0	Treatment	1	–	14.620	<b>&lt;0.001</b>
	s(plant material) : burned	1.000	1.000	11.505	<b>0.003</b>
	s(plant material) : unburned	3.966	4.815	3.342	<b>0.026</b>
Day-10	Treatment	1	–	9.680	<b>0.005</b>
	s(plant material) : burned	2.070	2.556	166.0	<b>&lt;0.001</b>
	s(plant material) : unburned	3.062	3.748	150.6	<b>&lt;0.001</b>
Day-31	Treatment	1	–	0.344	0.563
	s(plant material) : burned	2.661	3.267	51.80	<b>&lt;0.001</b>
	s(plant material) : unburned	3.495	4.261	23.07	<b>&lt;0.001</b>
Day-59	Treatment	1	–	2.476	0.129
	s(plant material) : burned	2.808	3.443	13.27	<b>&lt;0.001</b>
	s(plant material) : unburned	1.000	1.000	29.70	<b>&lt;0.001</b>
<b>Methane (nM)</b>					
Day-0	Treatment	1	–	2.038	0.166
	s(plant material)	1.000	1.000	0.718	0.405
Day-10	Treatment	1	–	0.266	0.611
	s(plant material) : burned	1.812	2.243	0.889	0.428
	s(plant material) : unburned	3.346	4.086	6.531	<b>0.001</b>
Day-31	s(plant material)	1	1.001	0.190	0.667
Day-59	Treatment	1	–	3.646	0.068
	s(plant material)	3.381	4.127	2.037	0.113

*Treatment* indicates the parametric term in GAM, *s(plant material)* is the smooth term for either burned or unburned treatments. *df*= degrees of freedom for parametric terms; *edf*= effective degrees of freedom for smoother terms; *Ref.df*= reference degree of freedom, where dashes indicate NA for parametric terms. Significant effects ( $p < 0.05$ ) are in bold.